ELSEVIER

Coordination Chemistry Reviews 144 (1995)
1–38

COORDINATION CHEMISTRY REVIEWS

High-valent oxomanganese clusters: structural and mechanistic work relevant to the oxygen-evolving center in photosystem II

Rajesh Manchanda, Gary W. Brudvig *, Robert H. Crabtree

Department of Chemistry, Yale University, P.O. Box 208107, New Haven, CT 06520-8107, USA

Received 7 January 1994; in revised form 27 February 1995

Contents

* Corresponding author.

SSDI 0010-8545(95)01147-1

Abstract

Recent years have seen a considerable interest in bioinorganic chemistry; in particular, the structural and functional modeling of active sites of metalloproteins. The oxomanganese tetramer in the O_2-evolving center (OEC) in photosystem II (PS II) of plants is thought to be the site of water oxidation to dioxygen. In conjunction with biophysical studies on the enzyme, inorganic chemists are trying to understand the structural and mechanistic aspects of the OEC by studying oxomanganese clusters. A number of such clusters, varying in nuclearity, ligation, and type and number of oxo-bridges, have been synthesized and characterized. Chemical, electrochemical and magnetic properties of these clusters have given much insight into the structure and function of the native enzyme. Here, we review recent efforts in inorganic model complex chemistry towards modeling the tetramanganese active site of PS II.

Keywords: Oxomanganese clusters; Photosystem II; Water oxidation

1. Introduction

One of the most important photochemical reactions in nature is the photosynthetic oxidation of water to dioxygen. This reaction is initiated by the incidence of light on the special chlorophyll, P_{680}, in the transmembrane protein complex called photosystem II (PS II). Subsequent oxidative steps of the oxomanganese cluster, known as the O_2-evolving center (OEC), result in the evolution of O_2 from water. With the structure of PS II still not determined, there have been intensive biophysical studies done on this enzyme. The information obtained by biophysical studies is used as a starting point for inorganic chemists, who are trying to model the active site of PS II. Inorganic modeling of the OEC in PS II is an area of active research. Researchers are synthesizing oxomanganese clusters with varying nuclearity, ligation and oxo-bridges. These systematic studies on oxomanganese clusters have been helpful in understanding some aspects of the native enzyme. Thus, there has been a productive interplay between the biophysical and inorganic studies.

With little structural information on the OEC, mimicking its chemical properties and structure is a challenge. In this review, we present the efforts in understanding the structure and function of the OEC by synthesis and study of oxomanganese model complexes. In particular, we focus our report on the various types of oxomanganese clusters synthesized to date and their physical properties.

This review is divided into six main sections. Section 2 deals with the background information on PS II, with emphasis on the OEC and its functioning. Inorganic chemists must base their efforts to model this metalloenzyme on the available information on the ligation, oxidation states and types of bridges between the metal centers. Also, mechanistic aspects of the enzyme are of great importance.

Section 3 is devoted to the various types of high-valent oxomanganese clusters, their structures and their relevance to the native enzyme. A number of tetranuclear Mn complexes have been prepared whose structures and properties can be compared to the various models proposed for the active site of the OEC. In addition, dinuclear and trinuclear complexes offer a reasonable starting point in understanding the chemistry of high-valent manganese and the behavior of the oxo-bridges under various conditions.

Section 4 covers the self-assembly of oxomanganese clusters and their aqueous chemistry. Conventional ligand design has been extended by the use of force fields modified to accommodate different metal centers. We also discuss this approach as applied to oxomanganese clusters.

The OEC cycles between different oxidation states of manganese, and oxidizes water to dioxygen. Electrochemical behavior of model complexes is thus important, and is discussed in Section 5.

Another interesting aspect of the OEC is its magnetic properties; the multiline EPR signal from the S_2 state of the OEC indicates an exchange-coupled system. The magnitude of this exchange gives valuable information on the structure. Section 6 discusses the magnetic properties of model complexes in light of the biophysical studies.

2. Photosystem II

2.1. Composition of PS II

PS II is an integral-membrane protein complex that is present in all organisms that carry out oxygenic photosynthesis (for review, see Refs. [1–4]). In plants, the chloroplast contains stacked membrane structures, called thylakoid membranes, that contain PS II. PS II is a large multi-subunit protein complex with a total mass of about 365 kDa (Fig. 1). There are two main subunits of about 32 kDa, known as D1 and D2, which form the photochemical core of PS II and are homologous to the L and M subunits of the structurally characterized bacterial reaction center [5]. The D1 and D2 subunits bind the redox centers involved in light-induced charge separation, which include the special chlorophyll (P_{680}), pheophytin and quinones, Q_A and Q_B. A non-heme iron is present in close vicinity to Q_A and Q_B. These components are collectively termed as the 'acceptor side', as electrons are shuttled through them from water in the photoactivated transport of electrons. D1 and D2 also contain the redox-active tyrosines Z (Y_Z) and D (Y_D) respectively, and it is likely that the oxomanganese cluster in the OEC is situated within these intrinsic subunits as well. The OEC and Y_Z comprise the 'donor side', providing electrons to reduce P_{680}^+. In two smaller polypeptides (about 10 and 6 kDa) associated with the D1 and D2 subunits, cytochrome b_{559} is located. The two other large, membrane-spanning subunits (43 and 47 kDa) shown in Fig. 1 bind chlorophylls that function as antennae to absorb light and transfer excitation energy to P_{680}.

Protruding from the lumenal side of the thylakoid membrane are three extrinsic

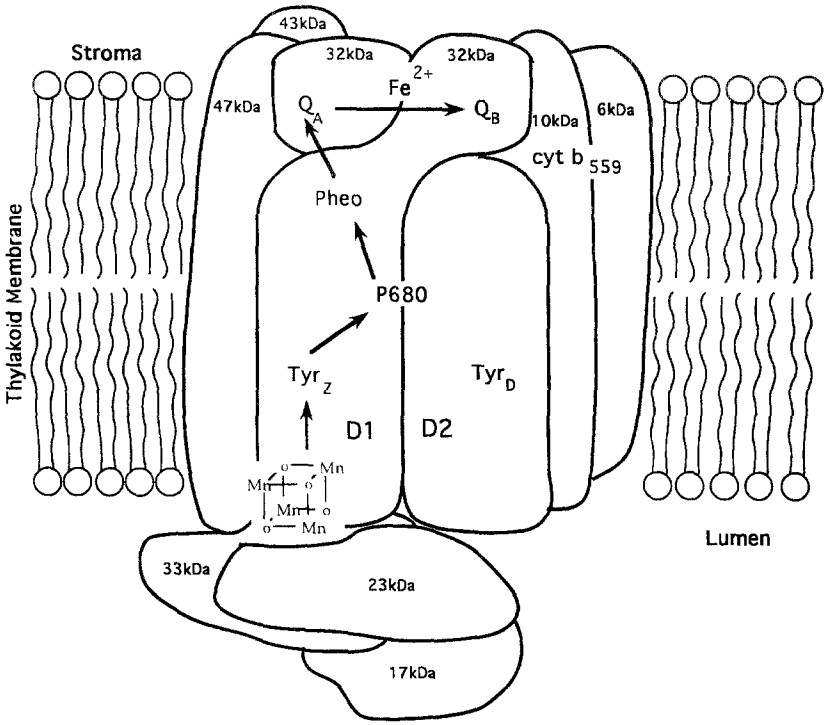

Fig. 1. Schematic representation of various subunits and redox-active components of PS II.

polypeptides. Their location is of importance, as it is believed that these polypeptides help shield the OEC from the aqueous medium. Of these three subunits, the 33 kDa polypeptide is closest to the OEC. Depletion of this subunit destabilizes the oxomanganese cluster, and manganese is easily lost from the OEC, with consequent loss of O_2 evolution. Two other extrinsic subunits, with molecular masses of 23 kDa and 17 kDa, also affect the stability of the OEC. Though the O_2-evolution activity of the enzyme is not affected, provided excess Ca^{2+} and Cl^- are present, the oxomanganese cluster is readily reduced by aqueous reductants after their depletion. This arrangement of the subunits and the specific location of the various redox centers in these polypeptides make PS II a highly complex system.

2.2. *Oxidation of water by the O_2-evolving center*

The O_2-evolving center (OEC) is capable of oxidizing water to dioxygen, which is a four-electron and four-proton reaction (Eq. (1)).

$$2H_2O \rightarrow O_2 + 4H^+ + 4e^- \quad (1)$$

The functioning of the OEC can be monitored by measuring the O_2 evolution with consecutive light flashes upon thylakoid membranes. The fact that every fourth flash

produced high yields of O_2 led Kok et al. [6] to propose a cyclic mechanism for the OEC (Fig. 2).

The primary photochemical reaction takes place at the special chlorophyll, P_{680}, resulting in a charge-separated state containing P_{680}^+. This oxidized state of P_{680} is reverted back to its photoactive reduced state by electron transfer from a neighboring tyrosine residue (Y_Z). The oxomanganese cluster donates an electron with each flash to reduce Y_Z^+ to Y_Z (Fig. 1) and cycles through a series of five oxidation states called S states. With every fourth flash, the oxomanganese cluster is oxidized enough to convert water to dioxygen.

O_2 evolution by PS II is dependent on various factors. It is imperative to have Ca^{2+} and Cl^- to observe any oxidation of water (for review, see Ref. [2]). These ions can be removed and substituted for by Sr^{2+} and Br^-, respectively, to regenerate O_2 evolution. Most other divalent cations and monovalent anions have been found to be ineffective in restoring O_2 evolution from PS II. The other important aspect is that water must bind to or in close vicinity of the oxomanganese cluster in order to get oxidized. The OEC sits in a hydrophobic pocket of the protein and thus water cannot access it so easily. There are suggestions that Ca^{2+} functions as the water-binding site located close to the oxomanganese cluster [7]. Competing molecules, e.g. ammonia [8], have been observed to alter the electron paramagnetic resonance (EPR) spectral characteristics of the manganese complex, indicating that this water analog binds to the manganese cluster in the S_2 state. It is still a matter of controversy where or when in the S-state cycle water binds to the OEC.

The other question to be answered is: what is the mechanism of the oxidation of water? It could be envisioned that the oxidation of water by the highly oxidized oxomanganese cluster could proceed via a concerted four-electron process or in two separate two-electron steps [9]. There is little evidence to support either pathway. No matter what the pathway, the concomitant release of protons is important. One

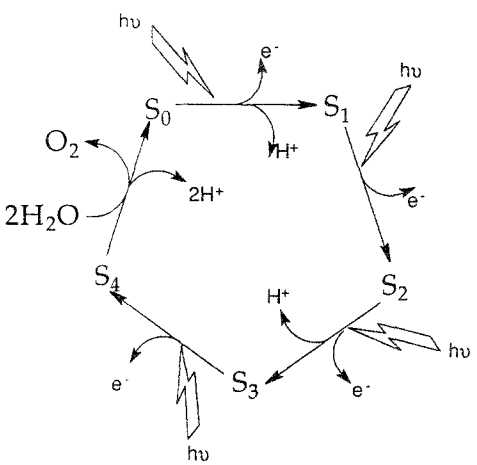

Fig. 2. Schematic diagram of Kok's S-state cycle showing different oxidation steps leading to oxidation of water.

way that the high-potential oxidized states of oxomanganese clusters can be stabilized is by deprotonation of bridging hydroxo-groups. This interplay of protonation/deprotonation with electron transfer is important in controlling the kinetic and thermodynamic stability of the cluster. Deprotonation of bridging hydroxo-groups with electron transfer has been proposed in the mechanistic models of Brudvig and Crabtree [10] and Christou and Vincent [11].

For O_2 to be formed, at least two water molecules have to be close to each other. Recent theoretical studies by Proserpio et al. [12] give information on the different mechanistic pathways and their relative activation parameters for O_2 evolution.

2.3. Manganese in PS II

As described above, the OEC is buried inside the protein structure and shielded from the aqueous phase by the extrinsic 33, 23 and 17 kDa polypeptides. It is not hard to envision that accessibility of various substrates is limited. From extended X-ray absorption fine structure (EXAFS) measurements, there has been some information on the ligation of the manganese ions in the OEC [13–15]. EPR [16] and electron spin echo envelope modulation (ESEEM) [17] measurements, in conjunction with site-directed mutagenesis studies, have given additional information on the ligation of the manganese ions and the possible locations of the manganese cluster in the PS II complex (reviewed in Ref. [4]).

The ligands to the OEC have to be oxidation-resistant and be able to accommodate conformational changes arising from any redox processes of the oxomanganese cluster. EXAFS data indicate that the first coordination shell of manganese is primarily O/N, although one S/Cl could be present, and that the coordination number is 5–6 [13–15]. ESEEM studies further indicate that the manganese ions do not have more than one or two nitrogen ligands, which, together with the EXAFS data, indicates that the manganese is in an oxygen-rich environment [17]. Recently, Tang et al. [18] prepared PS II with ^{15}N-labeled histidine residues. Then, by using ESEEM spectroscopy, it was found that there is at least one histidine ligating to manganese in the OEC. As for the other ligating residues, carboxylates are the likely candidates. Glutamic acid and aspartic acid could bind to manganese, but serine, tyrosine and threonine could bind as well. Another important aspect of the ligands is their ability to protonate/deprotonate. It is thought that the oxidative cycle of the OEC involves electron transfer concurrent with proton release.

The location of the Mn binding site in the PS II complex is still uncertain. However, site-directed mutagenesis studies have shown that several carboxylic acid and histidine residues are necessary for assembly and function of the Mn cluster [19]. These studies point to a location of the Mn cluster in the D1 subunit near the lumenal side of the membrane (Fig. 1).

The multiline EPR signal observed from the S_2 state of the OEC has been studied widely to understand the oxidation states and the conformation of the OEC [20]. There is also a $g=4.1$ EPR signal from the same state. For an EPR signal to be observed, the metal ions have to be magnetically coupled to give rise to a half-integral spin ground state. The multiline EPR signal is centered at $g=2$ and arises

from an $S=1/2$ ground spin state. On the other hand, the broad $g=4.1$ EPR signal can arise from an $S=3/2$ or $S=5/2$ spin state (Fig. 3).

These two EPR signals are interconvertible, leading to a model in which there are two different, interchangeable conformations of the tetranuclear oxomanganese cluster [21]. The two S_2-state EPR signals are explained by different exchange interactions between the manganese ions in each conformation. Analyses of the magnetic properties of exchange-coupled manganese tetramer models give some insight into the possible arrangement of the manganese ions in PS II [22]. A dimer-of-dimers model has been suggested to account for the S_2-state EPR signals [23].

2.4. Structure of the O_2-evolving center

The complexity of the membrane-bound PS II protein complex and difficulties in purifying PS II have resulted in the inability of researchers to grow good-quality single crystals. With no X-ray structure at hand, researchers have relied on other techniques, as described above, to get as much information as possible.

There have been intensive EXAFS studies conducted on the OEC in PS II. The groups of Penner-Hahn [14] and Sauer and Klein [15] have been active in this area. It has been concluded that there are two sets of metal–metal distances in the OEC: one of 2.7 Å and the other of 3.3 Å. Assignment of these has been a topic of much debate among different groups. The shorter metal–metal distance, 2.7 Å, fits well with a di-μ-oxo-bridged dimeric manganese unit.

EPR studies indicate a dimer-of-dimers arrangement of manganese in the OEC. The longer distance of 3.3 Å seen in the EXAFS could well be the distance between two such dimeric species. But again, EXAFS cannot easily distinguish between manganese and calcium. It is possible that the 3.3 Å distance corresponds to a manganese–calcium separation rather than a manganese–manganese dimer separa-

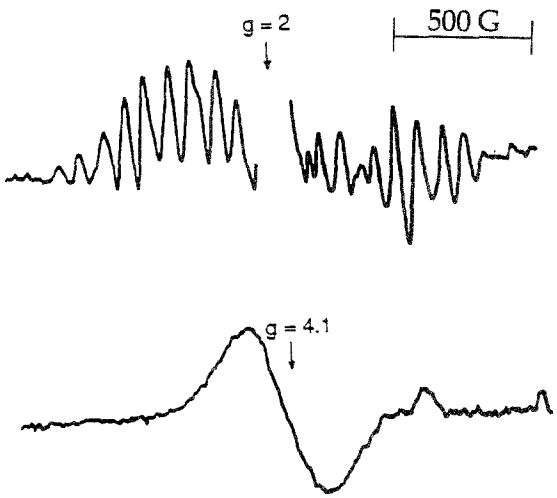

Fig. 3. Light-induced S_2-state EPR spectra from PS II membranes (adapted from Ref. [76]).

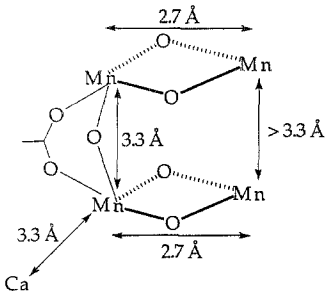

Fig. 4. Speculative model of the OEC in PS II, based on biophysical studies done by different groups.

tion. Calcium is essential for O_2 evolution, and it has been viewed as a structural component which stabilizes the OEC. Alternatively, if the calcium binding site is located at 3.3 Å from the Mn cluster, it could act as a water-binding site in the OEC. On the other hand, if it is supposed that the 3.3 Å separation is the distance between two manganese centers, then an oxo/carboxylate bridge could effectively fit the picture (Fig. 4).

Based on all the information from biophysical studies, various groups have put forth models for the OEC. There is no report of any manganese model complex capable of oxidizing water to dioxygen by the sequential uptake of oxidizing equivalents, as in PS II. Nevertheless there are high-valent oxomanganese clusters that exhibit structural features similar to those found in the natural system. Christou has isolated 'butterfly' complexes and has conducted intensive studies on carboxylato-bridged oxomanganese complexes [24]. The 'adamantane' oxomanganese cluster has been synthesized by Wieghardt et al. [25] with six μ-oxo bridges to four high-valent manganese ions. An intimately bound 'cubane' with apical chloro has also been isolated by Christou and co-workers [26]. Recently, Chan and Armstrong [27] synthesized a discrete 'dimer of dimers' complex with interesting structural properties resembling the proposed structure of the OEC. Girerd and co-workers [28,29] have been able to isolate a 'linear' oxo-bridged manganese tetramer with unusual structural and magnetic properties. These structures are summarized in Fig. 5. The next and more important step would be to attain reactivity similar to that of the natural system from tetranuclear oxomanganese clusters.

3. Assembly of oxomanganese clusters

Biophysical studies suggest that the OEC in PS II contains four manganese ions in higher oxidation states (Mn(III) or Mn(IV)). EXAFS and ESEEM data indicate a mostly O-donor ligation with at least one N-donor imidazole ligand. Support for a di-μ-oxo linkage between the Mn ions comes from the 2.7 Å distance observed in the OEC by EXAFS. Thus, in the modeling of the OEC, these structural requirements should be satisfied. For this purpose, understanding the chemistry of manganese in its higher oxidation states with various ligation spheres has proved helpful

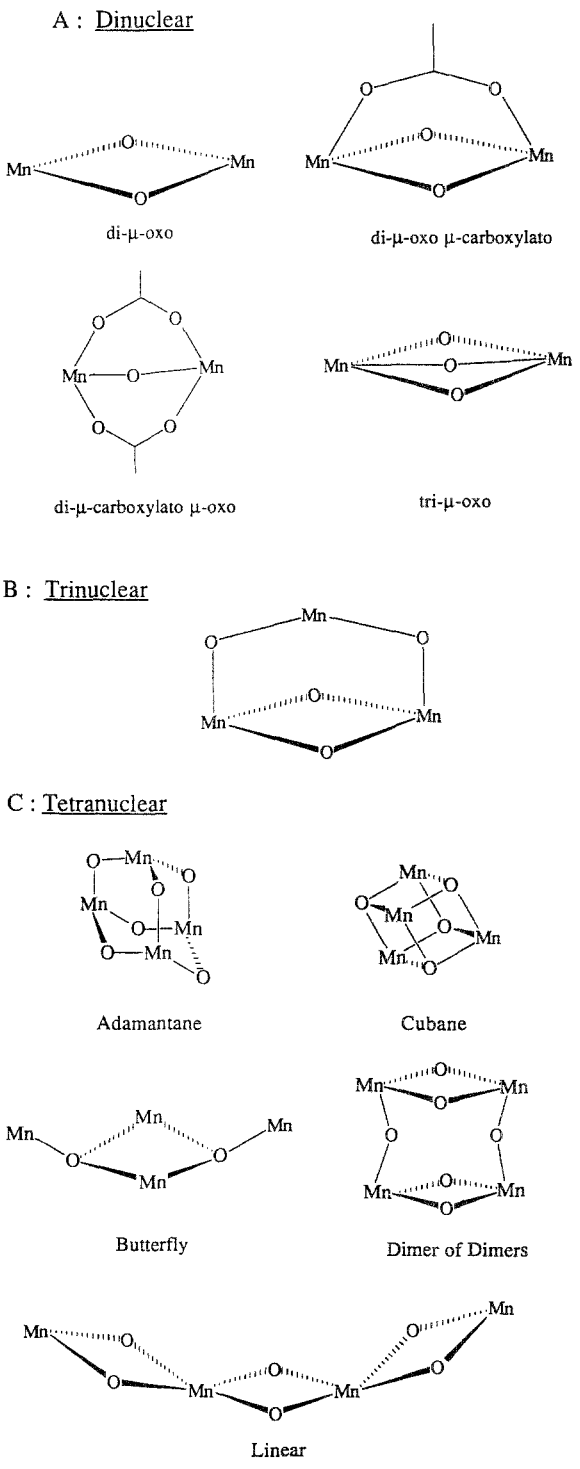

Fig. 5. Structural types of high-valent oxomanganese clusters: A, dinuclear; B, trinuclear; C, tetranuclear.

[24,30–32]. In this section, we review steps taken to synthesize oxomanganese clusters via different pathways, and novel approaches in designing ligands for such clusters. Lability of manganese in aqueous solution, resulting in equilibria between various species, is important mechanistically and is discussed below.

3.1. Preparation of oxomanganese clusters

Manganese has a rich chemistry in its various oxidation states [33]. It has an electronic configuration of $4s^2$ $3d^5$ and its more stable oxidation states include +2 (d^5), +3 (d^4), +4 (d^3) and +7 (d^0). Most of the high-valent Mn complexes that have been synthesized, and are discussed in the text, contain oxidation states of Mn(III) and Mn(IV). With Mn(II) being the most abundant source of manganese [33], it is obvious that the syntheses of high-valent oxomanganese clusters require a source of oxidizing equivalents, although there are preparations in which Mn is initially in a higher oxidation state [28]. In the literature, there is a plethora of such oxidizing reagents. The limiting factor in the use of many oxidants is the attainment of thermodynamic control over kinetic control. Even though the reduction potential of an oxidizing reagent is high, it may be kinetically inert towards reduction. In this regard, syntheses of oxomanganese complexes have utilized a wide variety of oxidants. Air is a rich source of dioxygen and has been used as the oxidizing agent in many preparations of oxomanganese clusters [34,35]. Bromine water and iodine have been employed and, lately, there has been an increase in the use of cerium(IV) [36] and also bromate. With Ce(IV) the reaction proceeds via a straightforward pathway involving simple electron transfer(s).

Yet another source of oxidizing equivalents is permanganate [37]. It has Mn in its +7 oxidation state with a standard reduction potential of 1.491 V. This potential is strongly pH-dependent. In aqueous preparations of oxomanganese clusters, potassium permanganate is used with acidic pH. For non-aqueous syntheses, [*n*-Bu_4N][MnO_4] has been employed [38]. Permanganate acts both as an oxidant and a source of manganese. Since there are two different oxidation states of Mn present in the reaction mixture, i.e. Mn(II) and Mn(VII), the stoichiometry of Mn(VII) is of importance.

Stabilization of higher oxidation states of Mn is the other issue. As stated above, carboxylates are good candidates for this purpose. Christou has done much of the work in this area [24]. Starting with a Mn_3O core with carboxylate bridges, an array of oxomanganese clusters have been developed. Oxo groups not only stabilize higher oxidation states, but are a necessity for modeling the OEC in PS II. The number of bridging oxo-groups is one of the determining factors in achieving a desired oxidation state of manganese. In aqueous preparations with the reaction mixture exposed to air, deprotonation of ligated water molecules is suspected to form oxo bridges. Template syntheses with either a pendant oxo-group or a preformed core as the starting material have also been widely used (for review, see Ref. [32]). Oxo transfer reagents and dioxygen from air are other sources of bridging oxo-groups.

The ancillary ligands also play a very important role in the formation and stability

of oxomanganese clusters. There is a large number of ligands ranging from bidentate to template polydentate that have been used in synthesizing oxomanganese clusters (Fig. 6). Ligands employed for preparations thus far are mostly nitrogen-based. These include aliphatic, cyclic, Schiff bases and polypyridyl systems.

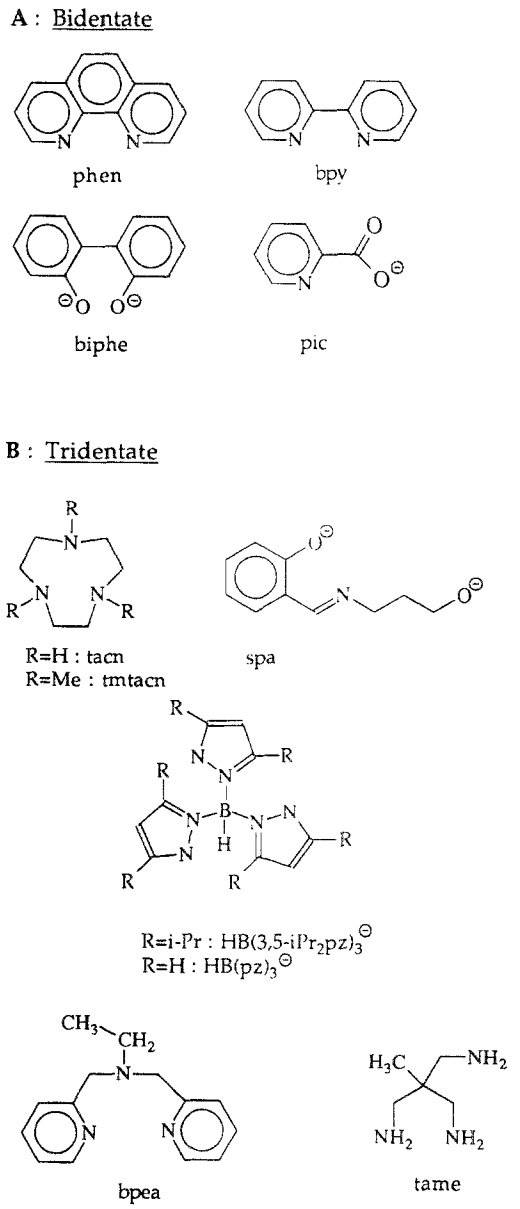

Fig. 6. Scheme of ligands used in the synthesis of high-valent oxomanganese clusters: A, bidentate; B, tridentate; C, tetradentate.

C : Tetradentate

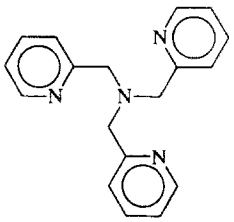

tmpa

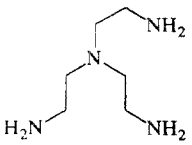

tren

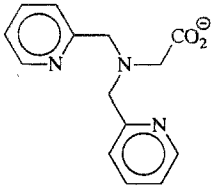

N_3O-py

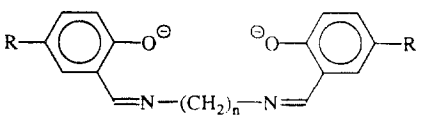

n= 2, R=H : salen
n= 2, R=Bu : Bu-salen
n= 3, R=Bu : Bu-saltn(Bu-salpn)

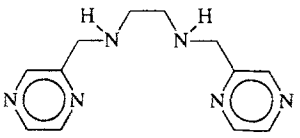

bispyzen

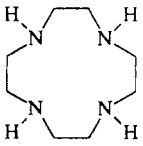

cyclen

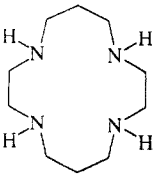

cyclam

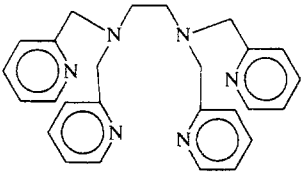

tpen

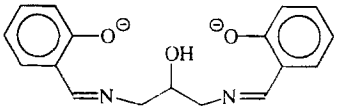

2-OH- salpn

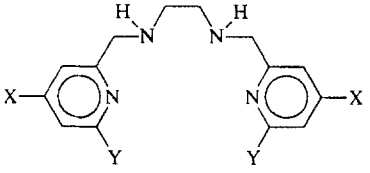

X=H, Y=H : bispicen
X=Me, Y=H : 4-Me_2-bispicen
X=H, Y=Me : 6-Me_2-bispicen

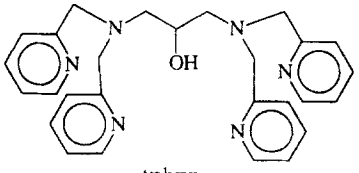

tphpn

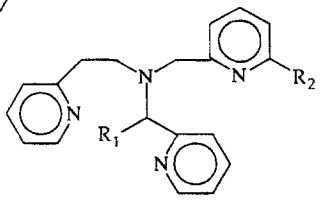

R_1=H, R_2=H : L1
R_1=CH_3, R_2=H : L2
R_1=H, R_2=CH_3 : L3

Even with a wide variety of ancillary ligands, it has been difficult to gain much control of the structure and/or oxidation state of the manganese center by controlling the geometry/electronic properties of the ligand. For example, there has been no example of a structurally characterized all oxygen-donor ligated oxomanganese dimer.

With little information on the ligation of the OEC in PS II, the ligands used for modeling work are based on trial and error. The rationale behind ligand usage has been mostly circumstantial; there is a need for a more systematic approach. There are new developments in the area of ligand design which are now beginning to gain interest.

3.2. Ligand design for oxomanganese clusters

Designing ligands is a novel approach towards gaining a better understanding of the ligand–oxometal relationship and its effect on geometry, electronic properties and reactivity of these complexes. It has been observed that the μ-oxo groups dictate the geometry around manganese centers in these complexes, and the remaining ligands have to accommodate to this constraint. For the past few decades, research in other areas of chemistry has utilized information obtained from structural data for previously reported complexes (for review, see Ref. [39,40]). These data, in turn, have been used to create force fields which define ideal bond lengths, bond angles, torsional angles, Van der Waals forces and electrostatic forces associated with various substructures in a molecule. This information is then converted into energy terms via force constants to give an estimate of the expenditure of energy required to perform a specific structural modification. It is thus comprehensible whether a molecule can be conformationally distorted or not. It is an aid to follow molecule–molecule interactions based on electrostatics or covalent linkages [41]. Drug design has relied heavily on these force fields to gain a better idea of drug-specific site interactions.

There are various examples of force fields, e.g. MM2 [42], CHARMM [43], AMBER [44], UFF [45], and many more, requiring different inputs and used for several different classes of molecules. For purely organic moieties, force fields have been effectively used and modified. On the other hand, it is only recently that there has been an upsurge in the use of force fields which take into account metal interactions. One problem in defining force fields for metals is the change in metal centers with oxidation/reduction. Another limiting factor is the number of complexes structurally characterized to be included in these empirical force fields. CHARMM [43] and UFF [45] are examples which can accommodate metal centers but are limited to only mononuclear metal complexes or multinuclear complexes in which all the metals have the same oxidation state. This is of little use in understanding the changes concomitant with a redox process.

We have been modifying Allinger's MM2 force field [42] to accommodate more than one metal center simultaneously with different oxidation states. MM2 is primarily an organic force field and normally allows one metal center. By systematic modifications using structural data on Mn(III) and Mn(IV) mononuclear complexes,

we have created a force field that can utilize parameters for Mn(III) or Mn(IV) [46]. With these parameters at hand, this force field can be used to study dimeric oxomanganese clusters with any class of ancillary ligands. The parameters developed for these complexes have been tested on structurally characterized complexes (Fig. 7). Thus, this modified MM2 force field accounts for energy changes from Mn(III) to Mn(IV), or vice versa, arising from structural modifications or electrostatic inter-actions.

This is a simple approach requiring parameters from reported complexes, and gives a fair idea about the feasibility of certain ligands and structural changes in these complexes upon a redox process. Structural information is important for these complexes, but dissolution in water often initiates structural rearrangements arising from chemical transformations of high-valent manganese.

3.3. Equilibria in aqueous solution

The OEC in PS II interacts with water during its photoactivated assembly and at least in the last stage of its oxidative cycle. It is thus relevant to study model complexes in aqueous media to gain insight into the chemistry of high-valent manganese in water. Assembly of high-valent oxomanganese clusters has been achieved in aqueous media owing to the fact that the manganese is a labile metal center allowing

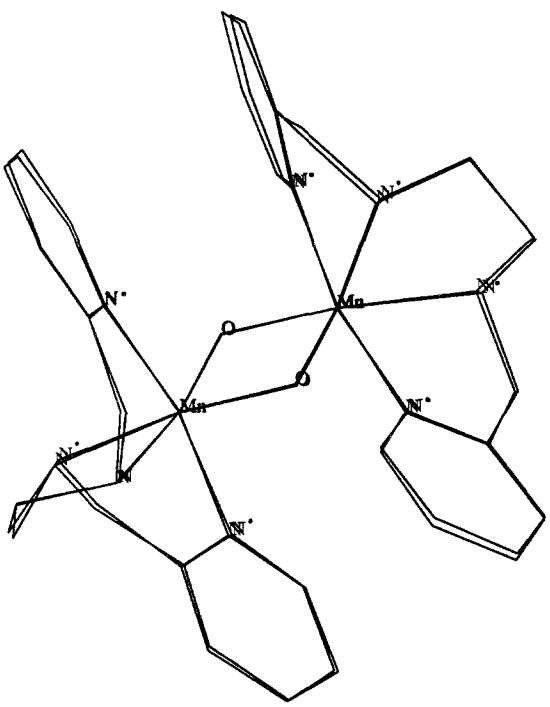

Fig. 7. Superimposition of the experimental crystal structure of $[Mn_2^{IV,IV}O_2(bispicen)_2]^{4+}$ and the structure obtained after energy minimization using a modified MM2 force field. Parameters of the modified MM2 force field and the minimization protocol have been described elsewhere [46].

several pathways for ligating species to stabilize it. Substitution of various ligands on Mn(III) can be achieved in aqueous solutions. The availability of vacant sites on a Mn center, in turn, allows for several different species to coexist in solution. Rapid rearrangements of these species lead to products with varying manganese–oxo and manganese–ligand ratios. This lability of manganese has led to several different isolable oxomanganese clusters from the same reaction mixture of Mn(II), bpy and acetate buffer [28,36,37,47,48].

The reaction of Mn(II) and Mn(VII) with bpy as the ancillary ligand leads not only to a Mn_2(III,IV) product [37] but to various other species that exist in the solution phase. Even dissolution of the $[Mn_2^{III,IV}O_2(bpy)_4]^{3+}$ dimer in an aqueous solution initiates a disproportionation reaction that is reversible upon addition of bpy [49]. Syntheses of many other carboxylato oxomanganese clusters depend on these solution equilibria [24]. Variation in the reaction conditions, such as ligand concentration, buffer, pH and even counter-ion, often leads to different isolable complexes [50].

Cooper and Calvin [37] studied the solution properties of simple dimeric oxomanganese clusters, $[Mn_2^{III,IV}O_2(bpy)_4]^{3+}$ and $[Mn_2^{III,IV}O_2(phen)_4]^{3+}$, but still researchers are finding new products from their reaction mixtures. A $[Mn_2^{IV,IV}(O)_2(phen)_4]^{4+}$ species can be isolated from an aqueous solution of its $Mn_2^{III,IV}$ dimer [37]. Also, $[Mn_2^{IV,IV}(O)_3(tmtacn)_2]^{2+}$ is formed from $[Mn_2^{III,III}(O)(OOCH_3)_2(tmtacn)_2]^{2+}$ upon dissolution in water [51]. It is not unusual that higher nuclearity clusters also fragment to yield smaller clusters, though the reverse has been observed more often. Dissolution of $[Mn_2^{IV,IV}O_2(OOCH_3)(bpea)_2]^{3+}$ in aqueous acetonitrile yields a trimeric oxomanganese species, $[Mn_3^{IV,IV,IV}O_4(OH)(bpea)_3]^{3+}$ [52].

Assembly of the OEC is thought to proceed via photo-oxidation of Mn(II) [53,54]. The stoichiometry of this process is still under debate, but it is believed that the initial two steps incorporate one Mn(III) ion with each flash and the next step is the uptake of two Mn(II) ions to assemble the tetrameric Mn complex. On the same lines, starting from a $[Mn^{III}(phen)(Cl)_3(H_2O)]$ species, it has been observed that a dimeric Mn_2(III,IV) species can be generated upon acidification [28]. In the case of $[Mn^{III}(bpy)(Cl)_3(H_2O)]$, the reaction is even more spectacular. It forms the usual dimeric species upon acidification, but further lowering of the pH yields a trimeric, $[Mn_3^{IV,IV,IV}O_4(bpy)_4(H_2O)_2]^{4+}$ species [48]. We have worked out the detailed mechanism of the transformation of the dinuclear species, $[Mn_2^{III,IV}O_2(bpy)_4]^{3+}$ to the trinuclear species, $[Mn_3^{IV,IV,IV}O_4(bpy)_4(H_2O)_2]^{4+}$ [49]. In the initial step, ligated bidentate bpy opens to a monodentate form with aqua ligands replacing bpy to form an observable intermediate. Auto-oxidation by another intermediate yields the trimeric species (Fig. 8).

Recently, Philouze et al. [28] isolated a linear Mn_4O_6 cluster by controlled acidification (to pH 2) of an aqueous solution of $Mn^{III}(bpy)(Cl)_3(H_2O)$. Hagen et al. [35] have observed protonation of an oxo group in the $[Mn_4O_6(tacn)_4]$ cluster upon lowering the pH.

Though it can be envisioned that there exist several equilibria in solution for these clusters, solubility and thermodynamics determine which of those species may be

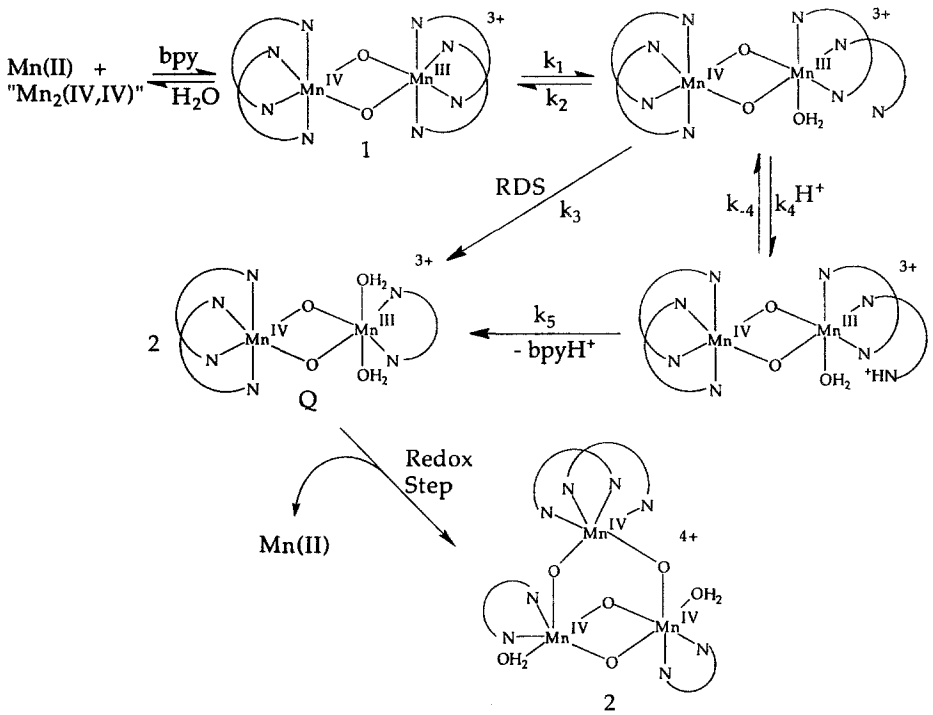

Fig. 8. Proposed scheme in the acid-induced transformation of $[Mn_2^{III,IV}O_2(bpy)_4](ClO_4)_3$ to $[Mn_3^{IV,IV,IV}O_4(bpy)_2(H_2O)_2](ClO_4)_4$ (adapted from Ref. [49]).

isolable. Solubility of these species can be altered either by changing the solvent system, in which case the least soluble thermodynamically stable species will precipitate first, or by varying the counter-ion. It has been observed [47] that, from the reaction mixture containing Mn(II), Mn(VII), acetate buffer and bpy, $[Mn_2^{III,III}O(OOCCH_3)_2(bpy)_2(H_2O)]^{2+}$ can be isolated by addition of NO_3^-, while $[Mn_2^{III,IV}O_2(bpy)_4]^{3+}$ is obtained with ClO_4^-. A recent report [36] indicates that yet another species, $[Mn_2^{IV,IV}O(OOCCH_3)_2(bpy)_2(H_2O)_2]^{3+}$, can be isolated from the same reaction mixture if perchloric acid is used. It is not only the counter-ions but also the buffer that take part in the interconversion of these various species. In most of the syntheses, acetate buffer is used but, depending on its concentration, it may coordinate as a bridging acetate or yield the desired μ-oxo product. Non-coordinating buffers have not been used extensively. Acidification of $[Mn_2^{III,IV}O_2(bpy)_4]^{3+}$ in phosphate buffer leads to a novel phosphato-bridged complex [55].

These various species observed in solution are in a redox-dependent equilibrium. In the absence of any external oxidant, it would seem probable that autoredox processes are in operation. This would indicate that higher valencies of manganese are not innocent. It is thus helpful to consider these equilibria in light of the valency of manganese, lability of ligands, pH and buffer in understanding manganese in the

OEC. Despite all these complex equilibria in solution, a wide variety of oxomanganese clusters have been isolated and structurally characterized.

4. High-valent oxomanganese clusters

In structural and functional modeling of the active site of a metalloenzyme, the aim is to mimic its structure and reactivity outside the protein. It is not easy to achieve this goal, since the protein supports the active center in a highly specific geometry which allows the metalloenzyme to achieve maximum catalytic activity. The protein backbone also accommodates changes in the structure around the metal center, arising from redox activity, by adjusting protein-folding. It is therefore a challenge to design ligands that could hold metals in a similar way and at the same time allow for redox changes at the metal center. In this respect, modeling of the OEC in PS II has met with little success. Instead of trying to aim for the synthesis of the active center, it is only prudent to design ligands and study model complexes with varying nuclearities to understand better the chemistry of the metal centers as well as the role of ancillary ligands.

4.1. Dinuclear complexes

There have been many reports on structurally characterized dinuclear high-valent oxomanganese complexes (for review, see Refs. [24,31,32,56]). Based on these, dinuclear oxomanganese complexes can be divided into four major categories: (a) di-μ-oxo, (b) di-μ-oxo μ-carboxylato, (c) μ-oxo di-μ-carboxylato, and (d) tri-μ-oxo. The structural characteristics of each of these species are dependent on the type of the bridge. Ancillary ligands for these complexes range from simple bidentate to pendant-type multidentate amino/hydroxy/carboxy compounds (Fig. 6). The stabilization of high valency of manganese centers is achieved in all these complexes as well.

4.1.1. Di-μ-oxo

High-valent oxomanganese dimers with two bridging oxo units were synthesized and studied much earlier for their unusual magnetic properties. The recent surge in studying them stems from the observation of a 2.7 Å distance in PS II, with implications that the manganese ions are strongly exchange-coupled. A similar distance has also been observed for the superoxidized state of Mn-catalase [57,58]. All of the common stable higher oxidation states (i.e. III,III; III,IV; IV,IV) of manganese have been achieved in these dimeric complexes. The most intriguing aspect of these complexes is the fact that the inter-metal distance remains almost constant (about 2.6–2.7 Å) with the change in oxidation state of manganese. The timescale of inter-metal electron transfer is slow and is obvious as seen by the X-ray crystal structure data. The manganese ions have trapped valences, and are found in their characteristic coordination in accordance with their oxidation state. In the Robin and Day scheme for mixed-valent complexes, these complexes are classified as type I. Thus, for Mn(III) (d^4) it is expected that there will be a Jahn–Teller distortion along the z axis, as is

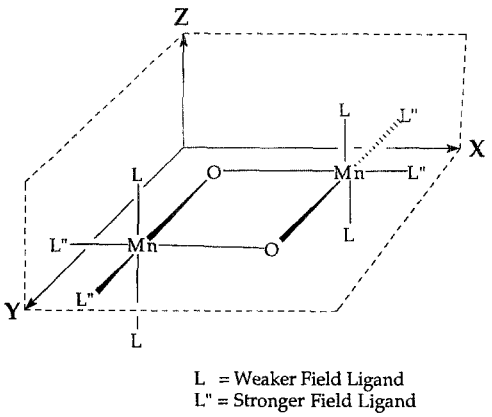

Fig. 9. Axial orientation of the di-μ-oxo manganese unit with the Mn–$(O)_2$–Mn plane parallel to the x–y plane. The stronger donating ligands are also oriented in the x–y plane.

observed (Fig. 9). The di-μ-oxo group seems to involve d-orbitals along the x–y plane resulting in axial distortions on the ligand. A simple molecular orbital picture has been presented elsewhere to account for this behavior [31]. It also implies that the di-μ-oxo group is a stronger-field ligand directing other stronger-field ligands trans to the μ-oxo groups (Fig. 9).

The rigidity of this oxo–metal plane is obvious from crystal structures, where it is observed that the plane containing the Mn-di-μ-oxo-Mn unit is least angularly distorted. Thus, the ancillary ligands in these complexes have to accommodate any structural adjustments arising from the rigid di-μ-oxo plane. In fact, the distances from metal to ancillary ligand show a clear trend of lengthening/shortening depending on the oxidation state of manganese.

4.1.2. Di-μ-oxo μ-carboxylato

Formation of a di-μ-oxo species in aqueous medium with acetate as the buffer has been found to go via an intermediate with a di-μ-oxo mono-μ-acetato structure [47]. As opposed to di-μ-oxo dimers, the additional bridging carboxylate results in shortening of the Mn–Mn distance to about 2.6 Å. The arguments presented in Ref. [31] for the orbital symmetry arising from the di-μ-oxo moiety hold for these complexes as well. The known examples either have III,IV or IV,IV oxidation states of manganese. Recently, an unusual dimer was reported [36] with water molecules coordinated to Mn(IV) in a di-μ-oxo mono-μ-carboxylato complex. The water molecules are trans to each other and, as discussed above, lie in the plane of the di-μ-oxo group. This is the first example of such a complex. Previously, a Mn(III,III) complex with chloro coordination to the Mn has been reported [24]. Also, Jahn–Teller distortions manifest in the axial metal-to-ligand bonds for Mn(III) in these complexes.

4.1.3. μ-Oxo di-μ-carboxylato

It is hypothesized that there are a few carboxylate bridges in the OEC of PS II. Carboxylate bridges are difficult to oxidize and are thus suitable for stabilizing high-

valent manganese. The presence of a μ-oxo bridge facilitates stabilization of high-valent manganese as well. Typically the Mn–Mn distances in these complexes have been found to be 3.1–3.2 Å (Table 1). The μ-oxo bridge in most of these complexes

Table 1
Oxidation states and inter-metal distances in dinuclear complexes

Complexes	Oxidation states	Mn–Mn (Å)	Ref.
Di-μ-oxo			
$[Mn_2O_2(HB(3,5\text{-}iPr_2pz)_3)_2]^0$	III, III	2.696	[81]
$[Mn_2O_2(6\text{-}Me_2bispicen)_2]^{2+}$	III, III	2.676	[82]
$[Mn_2O_2(6\text{-}Me_2tmpa)_2]^{2+}$	III, III	2.674	[82]
$[Mn_2O_2(bispyzen)_2]^{2+}$	III, III	2.686	[82]
$[Mn_2O_2(bispicen)_2]^{3+}$	III, IV	2.659	[83]
$[Mn_2O_2(bpy)_4]^{3+}$	III, IV	2.716	[84]
$[Mn_2O_2(cyclam)_2]^{3+}$	III, IV	2.741	[85]
$[Mn_2O_2(HB(3,5\text{-}iPr_2pz)_3)_2]^+$	III, IV	2.696	[81]
$[Mn_2O_2(L1)_2]^{3+}$	III, IV	2.693	[86]
$[Mn_2O_2(L2)_2]^{3+}$	III, IV	2.682, 2.702	[86]
$[Mn_2O_2(N_3O\text{-}py)_2]^{3+}$	III, IV	2.656	[87]
$[Mn_2O_2(phen)_4]^{3+}$	III, IV	2.700	[88]
$[Mn_2O_2(tmpa)_2]^{3+}$	III, IV	2.643	[89]
$[Mn_2O_2(tren)_2]^{3+}$	III, IV	2.679	[34]
$[Mn_2O_2(bispicen)_2]^{4+}$	IV, IV	2.672	[82]
$[Mn_2O_2(bpy)_2(\mu\text{-}HPO_4)(H_2PO_4)_2]^0$	IV, IV	2.702	[55]
$[Mn_2O_2(L3)_2]^{4+}$	IV, IV	2.747	[82]
$[Mn_2O_2(phen)_4]^{4+}$	IV, IV	2.748	[88]
$[Mn_2O_2(pic)_4]^0$	IV, IV	2.747	[79]
$[Mn_2O_2(salpn)_2]^0$	IV, IV	2.720	[90]
$[Mn_2O_2(tmpa)_2]^{4+}$	IV, IV	na	
Di-μ-oxo μ-carboxylato			
$[Mn_2O_2(O_2CCH_3)(bpy)_2Cl_2]^0$	III, IV	2.667	[24]
$[Mn_2O_2(O_2CCH_3)(tmtacn)_2]^{2+}$	III, IV	2.588	[51,91]
$[Mn_2O_2(O_2CCH_3)(tpen)]^{2+}$	III, IV	2.591	[52]
$[Mn_2O_2(O_2CCH_3)(bpy)_2(H_2O)_2]^0$	IV, IV	2.642	[36]
$[Mn_2O_2(O_2CCH_3)(bpea)]^{3+}$	IV, IV	2.580	[52]
μ-oxo di-μ-carboxylato			
$[Mn_2O(O_2CCH_3)_2(bpy)_2(H_2O)_2]^{2+}$	III, III	3.153	[92]
$[Mn_2O(O_2CCH_3)_2(bpy)_2(N_3)_2]^0$	III, III	3.153	[24]
$[Mn_2O(O_2CCH_3)_2(HB(pz)_3)_2]^0$	III, III	3.159	[93]
$[Mn_2O(O_2CCH_3)_2(tmip)_2]^{2+}$ [a]	III, III	3.164	[94]
$[Mn_2O(O_2CCH_3)_2(tmtacn)_2]^{2+}$	III, III	3.084	[51]
Tri-μ-oxo			
$[Mn_2O_3(tmtacn)_2]^{2+}$	IV, IV	2.296	[51]
Di-μ-oxo μ-peroxo			
$[Mn_2O_2(O_2)(tmtacn)_2]^{2+}$	IV, IV	2.531	[59]

[a] tmip = tris-(imidazol-2-yl)phosphine.

is linear, with the carboxylates spanning the plane of the manganese–oxo bond. It would require a tridentate ligand to accommodate such a configuration, but complexes containing bidentate and monodentate ligands have also been characterized. The x–y plane in these complexes is not as well supported as in the above cases, resulting in the flexibility of the linear metal–oxo bond.

4.1.4. Tri-μ-oxo

There has been only one report of a tri-μ-oxo manganese (IV,IV) complex by Wieghardt et al. [51]. As expected, the metal–metal distance is extremely short (about 2.296 Å). The supporting ligand is an aliphatic cyclic nitrogen-donor tridentate ligand, tmtacn. The short Mn–Mn distance rules out this type of structural unit in the OEC. On the other hand, the unusual magnetic properties arising from this complex will be discussed later.

There is one example of a μ-peroxo di-μ-oxo dimeric complex. Bossek et al. [59] isolated a Mn(IV,IV) complex with a peroxo bridge and a di-μ-oxo unit. It is of importance in modeling the OEC, as it is envisioned that the elusive S_4 state in the water oxidation cycle may proceed via a peroxo intermediate. This is the first such example of high-valent manganese bridged via a peroxo group. It also demonstrates the versatility of tmtacn as a tridentate ligand. The Mn–Mn distance in this complex is 2.531 Å and it is in the range expected for a di-μ-oxo manganese moiety.

4.2. Trinuclear complexes

Oxomanganese carboxylate trinuclear compounds (basic acetates) have been known for almost a century [60]. Although they hold no relevance to PS II, they have proved useful as starting materials for synthesizing various other types of oxomanganese clusters [24]. On the other hand, a number of trinuclear oxomanganese clusters of a more promising type have been reported. Auger et al. [61] reported a complex, $[Mn_3^{IV,IV,IV}O_4(Cl)_2(bpy)_4](MnCl_4)$, with a di-μ-oxo Mn(IV) dimer coordinated to two chlorides, and each manganese of this basal dimer bound via a μ-oxo bond to an apical Mn(IV). The Mn-to-O ratio of 3:4 and high valency of Mn in this complex were of relevance to PS II. More interesting were the inter-metal distances; the dimeric manganese ions are separated from the apical manganese at 3.243 Å, and the inter-metal distance in the basal dimer was 2.681 Å. These distances are close to those observed in the OEC. Sarneski et al. [48] isolated a structurally similar (Mn–Mn 2.679 Å and 3.254 Å) complex but, instead of chlorides, water was bound to each of the basal manganese(IV) ions. This was the first example of water coordinated to high-valent manganese without any supporting carboxylates. The aqua (and chloro) ligands were located trans to one another. As explained above, the di-μ-oxo plane in the basal dimer dictates the geometry around the metal centers in these complexes as well.

More recently, Armstrong reported [52] a similar trinuclear complex, $[Mn_3^{IV,IV,IV}O_4(OH)(bpea)_3](ClO_4)_3$; it has a monodentate hydroxo ligand coordinated to the apical Mn ion. This hydroxo ligand can easily be replaced by other monodentate ligands such as fluoride, chloride, isocyanide or a water molecule. The

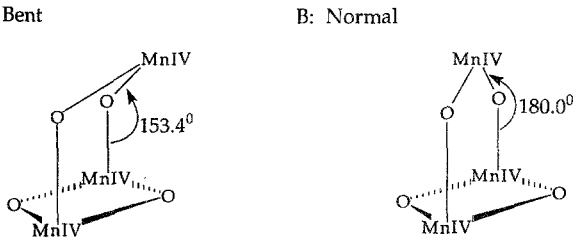

Fig. 10. Schematic diagram of two different types of trinuclear oxomanganese clusters: A, bent; B, normal.

other unusual structural aspect of this complex is the 'bend' at the μ-oxo linkage in the oxomanganese planes between basal (Mn ions bound to each other via a di-μ-oxo bridge) and apical (Mn ion bound to each of the basal Mn via a μ-oxo bridge) manganese units (Fig. 10). In the previous two examples [48,61], the angle between these two planes was found to be close to 0°, but in Armstrong's complex this angle is increased to 26.6° (Fig. 10). The implications of this 'bend' and the coordinated apical ligand on the magnetic properties of the complex are discussed below.

4.3. Tetranuclear complexes

Like the dinuclear complexes discussed above, tetranuclear complexes can also be divided into structurally distinct classes. Each of these classes has a unique geometrical configuration with a fixed manganese–oxo ratio. There are at least five such classes: (a) butterfly, (b) adamantane, (c) cubane, (d) linear and (e) dimer of dimers (Fig. 5C). The importance of tetranuclear complexes is due to the fact that the OEC contains four manganese atoms per cluster. We have not included oxomanganese clusters with manganese in lower oxidation states (e.g. II,II,II,II; II,II,II,III; II,II,III,III; II,III,III,III) or tetrameric structures as a unit of a higher nuclearity cluster in our discussions.

4.3.1. Butterfly

These types of clusters are characterized by the presence of a central dimeric di-μ_3-oxo manganese unit coordinated to two outer manganese atoms at each of the oxo groups, giving a Mn_4O_2 unit. The butterfly complexes have been isolated with various bridged carboxylates and terminal ligands. Vincent et al. [62] have synthesized a carboxylate-bridged Mn(III) cluster with two sets of Mn–Mn distances (2.848 Å and 3.299 Å). Another similar mixed-valent complex with two Mn(II) and two Mn(III) has also been isolated. Kulawiec et al. [63] isolated a butterfly-type cluster with all-oxygen coordination. The inter-metal distances in this complex (2.776 Å and 3.265 Å) and its all-oxygen coordination sphere make it an important model for comparison to the OEC, but the average oxidation state of 2.5 is too low.

4.3.2. Adamantane

This type of tetranuclear cluster is characterized by a Mn:Oxo ratio of 4:6, arranged via six μ-oxo bonds between the manganese ions. The average distance

between Mn ions is found to be about 3.2 Å. This type of geometry requires the ligand to be tridentate and facial. Tacn and tame both give structurally characterized adamantane-type clusters [35,51].

Deprotonation of the OEC is an important aspect in its oxidative cycle (Fig. 2). Structural changes concomitant with protonation of an oxo-group have been observed in adamantane-type clusters. There are obvious structural and magnetic manifestations of protonation of an oxo-group. An average change of about 0.18 Å in the distances between Mn ions upon protonation has been observed [35]. Magnetic changes arising from this transformation will be discussed later.

4.3.3. Cubane

There are no examples of tetranuclear oxomanganese clusters with a symmetric cubane-type geometry and the appropriate manganese-to-oxo ratio. It is required that there should be four Mn ions and four oxo groups in an intimately magnetically coupled system to yield a cubane. But, to date, only a cobalt–oxo cube has been characterized [64], which has the required geometry and metal-to-oxo ratio needed for an oxomanganese cube. (There are examples of cubane-type Mn clusters as smaller units in a larger Mn–oxo cluster [24].) The examples of cubane-type tetranuclear oxomanganese clusters are limited to four manganese with three μ_3-oxo bridges and one apical μ_3-halo (chloro/bromo) bridge [65,66]. Three of the four manganese atoms are in the +3 oxidation state, with the fourth in the +4 state. The distance between the μ-oxo bridged Mn(III) ions is about 2.7 Å, with a longer Mn(III)-to-Mn(IV) chloro-bridged bond (about 3.3 Å). Recently Gedye et al. [67] have isolated another structurally distinct oxomanganese tetramer with an open fused cubane geometry. Interconversion of cubane to adamantane with concomitant deprotonation/protonation has been proposed as a possible pathway for the oxidative cycle of the OEC by Brudvig and Crabtree [10] and expanded by Brudvig and de Paula [68].

4.3.4. Linear

There are several examples of linear manganese complexes, but mostly with coordinated carboxylates or with Mn(II). Only recently, Girerd and co-workers [28] isolated an unusual linear oxomanganese cluster, $[Mn_4^{IV,IV,IV,IV}O_6(bpy)_4](ClO_4)_4$. It has a Mn:oxo ratio of 4:6, with all of its manganese ions in the +4 state. Each Mn is coordinated to another Mn via a di-μ-oxo bridge. This arrangement gives a highly unusual configuration around two central Mn ions; each of these Mn(IV) now has four oxo groups! As expected for any Mn-di-μ-oxo-Mn unit, the Mn–Mn distance is close to 2.7 Å. The central Mn ions are coordinated to one bpy each, while the outer Mn ions have two bpy ligands. This complex exhibits unique magnetic properties.

4.3.5. Dimer of dimers

It is thought that the OEC has a configuartion with two Mn dimers interacting with one another. A cubane can be thought of as one example of this configuration, although a symmetric cubane does not appear to fit with the biophysical observations. Chan and Armstrong [27] reported a dimer-of-dimers complex,

$[(Mn_2^{III,IV}O_2)_2(tphpn)_2](ClO_4)_4$, with two di-$\mu$-oxo manganese dimers linked to each other via a pendant-μ-alkoxo bond. There are two distances observed: the shorter Mn–Mn distance is 2.654 Å, corresponding to the Mn–Mn in a di-μ-oxo moiety, and a longer distance of 3.971 Å that is the separation between the two such dimeric units. The ligand tphpn coordinates side-on, facilitating its pendant hydroxo group to link two dimers at a fixed distance, while the pyridyl groups on the ligand coordinate in a facial fashion. In light of all these structurally characterized oxomanganese clusters, it is essential to investigate their thermodynamic properties.

5. Electrochemical properties

Electrochemical properties of transition metals reflect the electronic behavior of the metal itself together with the effects of ancillary ligands, solvent, temperature and pH. This holds relevance to mechanistic aspects of the OEC and its S-state cycle. The electrochemical behavior of model complexes shows the thermodynamics of the system under various conditions. By understanding this behavior, it may be possible to suggest pathways via which the metal center in the native enzyme may be functioning. We discuss electrochemical behavior in non-aqueous solvents, followed by the implications of employing aqueous media for these measurements.

5.1. Effect of ancillary ligands

Apart from the metal center itself, the immediate ligation sphere around the metal contributes to the stabilization of different oxidation states of the metal. Further, the direct effect of electron-donating/electron-withdrawing capabilities of the ancillary ligands is important in attaining higher oxidation states. These effects can be measured readily by cyclic voltammetry. Oxidation of water to dioxygen is a four-electron, four-proton process (the reduction potential for this reaction is 1.55 V(NHE) under standard conditions and is pH-dependent); for any model oxomanganese complex to oxidize water, it has to have a reduction potential as high as this. With different ancillary ligands, the presence of oxo groups and carboxylates makes it possible to attain high-valence states of manganese. As shown in Table 2, there is a wide range of electrochemical potentials for oxomanganese clusters. For a simple case like the dimers, the effect of ancillary ligands is obvious. For most of the cases discussed, the initial oxidation states of manganese are III,III. These dinuclear III,III complexes can be oxidized to their one-electron oxidized form, i.e. III,IV, and further to a two-electron oxidized IV,IV form. These transformations are easily accessible in di-μ-oxo complexes and, also, in the μ-oxo di-μ-carboxylato tmtacn complex, and they proceed via sequential one-electron steps.

The reduction potential and stability of the higher oxidation states in these complexes is, as expected, dependent on the donor properties of the ancillary ligands. For example, in the case when an all-pyridine ligation (tmpa) is present, the reduction potential is much higher than for a more donating ligand with a terminal carboxylate trans to the μ-oxo group (N_3O-py) (Table 2). This trend of lowering of the reduction

Table 2
Exchange coupling parameters and reduction potentials for dinuclear complexes

Complexes	Oxidation states	J (cm^{-1})[a]	$E_{1/2}$[b] (III,III/III,IV)	$E_{1/2}$[b] (III,IV/IV,IV)	Ref.
Di-μ-oxo					
$[Mn_2O_2(6\text{-}Me_2bispicen)_2]^{2+}$	III, III	172	0.57	1.34	[82]
$[Mn_2O_2(6\text{-}Me_2tmpa)_2]^{2+}$	III, III	na	0.68	1.45	[82]
$[Mn_2O_2(bispyzen)_2]^{2+}$	III, III	na	na	na	[82]
$[Mn_2O_2(bispicen)_2]^{3+}$	III, IV	280	0.14	0.75	[83]
$[Mn_2O_2(bpy)_4]^{3+}$	III, IV	300	0.29	1.25	[84]
$[Mn_2O_2(cyclam)_2]^{3+}$	III, IV	na	−0.12	1.00	[85]
$[Mn_2O_2(L1)_2]^{3+}$	III, IV	na	0.23	1.03	[86]
$[Mn_2O_2(L2)_2]^{3+}$	III, IV	na	0.26	1.16	[86]
$[Mn_2O_2(L3)_2]^{3+}$	III, IV	353	na	na	[86]
$[Mn_2O_2(L4)_2]^{3+}$	III, IV	442	0.38	1.28	[86]
$[Mn_2O_2(N_3O\text{-}py)_2]^{3+}$	III, IV	302	−0.02	0.76	[95]
$[Mn_2O_2(phen)_4]^{3+}$	III, IV	268	0.33	1.29	[88]
$[Mn_2O_2(tmpa)_2]^{3+}$	III, IV	318	0.24	1.04	[89]
$[Mn_2O_2(tren)_2]^{3+}$	III, IV	292	0.08	0.83	[34]
$[Mn_2O_2(bispicen)_2]^{4+}$	IV, IV	251	na	1.00	[82]
$[Mn_2O_2(bpy)_2(\mu\text{-}HPO_4)(H_2PO_4)_2]^0$	IV, IV	79	na	0.70	[55]
$[Mn_2O_2(L3)_2]^{4+}$	IV, IV	262	0.49	1.32	[82]
$[Mn_2O_2(phen)_4]^{4+}$	IV, IV	288	na	na	[88]
$[Mn_2O_2(pic)_4]^{4+}$	IV, IV	174	−0.47	0.66	[79]
$[Mn_2O_2(salpn)_2]^0$	IV, IV	134	na	−0.39	[90]
$[Mn_2O_2(tmpa)_2]^{4+}$	IV, IV	274	na	1.20	[82]
Di-μ-oxo μ-carboxylato					
$[Mn_2O_2(O_2CCH_3)(bpy)_2Cl_2]^0$	III, IV	228	na	na	[24]
$[Mn_2O_2(O_2CCH_3)(tmtacn)_2]^{2+}$	III, IV	440	na	na	[51,91]
$[Mn_2O_2(O_2CCH_3)(tpen)]^{2+}$	III, IV	na	na	0.90	[50]
$[Mn_2O_2(O_2CCH_3)(bpy)_2(H_2O)_2]^0$	IV, IV	134	na	na	[36]
$[Mn_2O_2(O_2CCH_3)(bpea)]^{3+}$	IV, IV	248	na	0.93	[52]
μ-oxo di-μ-carboxylato					
$[Mn_2O(O_2CCH_3)_2(bpy)_2(H_2O)_2]^{2+}$	III, III	6.8	na	na	[92]
$[Mn_2O(O_2CCH_3)_2(bpy)_2(N_3)_2]^0$	III, III	−6.8	na	na	[24]
$[Mn_2O(O_2CCH_3)_2(HB(pz)_3)_2]^0$	III, III	1.0	0.82	1.53	[93]
$[Mn_2O(O_2CCH_3)_2(tmip)_2]^{2+c}$	III, III	0.5	0.59	na	[94]
$[Mn_2O(O_2CCH_3)_2(tmtacn)_2]^{2+}$	III, III	−18	0.89	1.51	[51]
Tri-μ-oxo					
$[Mn_2O_3(tmtacn)_2]^{2+}$	IV, IV	770	na	na	[51]
Di-μ-oxo μ-peroxo					
$[Mn_2O_2(O_2)(tmtacn)_2]^{2+}$	IV, IV	na	na	na	[59]

[a] $H_{ex} = J(S_1S_2)$.
[b] Potentials are in volts vs. SCE.
[c] tmip = tris-(imidazol-2-yl)phosphine.

potential continues as the donating capability of the ligand is increased. Of all the ligands systems available for di-μ-oxo manganese dimers, salpn stabilizes the IV,IV state to a great extent ($E_{1/2} = -0.39$ V(SCE) for the IV,IV/III,IV couple). The dominant donor in this case is the terminal phenoxy group on each manganese center trans to the di-μ-oxo unit.

The other extreme in which the IV,IV state is least stabilized is with pyrazine-based ligands (bispyzen), while other examples include pyridine-based ligands (Me_2-tmpa, L2, L3, 6-Me_2bispicen). Reversibility of the redox processes in these complexes is dependent on the structural flexibilty and electronic nature of the ancillary ligands. Yu et al. [69] have been able to demonstrate a four-electron redox process in an alkoxy-bridged dinuclear complex, $[Mn_2(salmp)_2]^{2-}$, (salmp = 2-(bis(salicylidieneamino)methyl)phenolate(3−)). Starting from a II,III oxidation state, this complex can undergo one-electron reduction to a II,II state or oxidation to a IV,IV state.

5.2. *Redox processes in higher-nuclearity clusters*

Stabilization of higher oxidation states of dinuclear manganese centers is important but, on the other hand, isolable lower oxidation states of Mn must be accessible within reasonable potentials for the complex to cycle between various oxidation states. Also, there has been no example (in dinuclear systems) where each Mn center undergoes a two-electron redox process, resulting in an overall four-electron redox process. Higher-nuclearity clusters (trimers, tetramers) offer answers to these problems. With more than two manganese centers, it is conceivable that, with each center undergoing a one-electron redox step, a four-electron redox process can be achieved. These sequential reduction potentials for higher-nuclearity complexes cover a wide range and are reasonably accessible. Although there is also no example of a two-electron redox step in these higher-nuclearity complexes, they offer sequential one-electron potentials that are close to each other.

In $[Mn_3^{IV,IV,IV}O_4(bpy)_4(H_2O)_2]^{4+}$, reduction by one electron at 0.36 V(SCE) is irreversible [48]. Reversible reduction corresponding to the IV/III couple has been observed in $[Mn_3^{IV,IV,IV}O_4(OH)(bpea)_3]^{3+}$; the authors [52] attribute this reduction ($E_{1/2} = 0.05$ V(SCE)) to the apical Mn(IV). Further reduction leads to an irreversible wave at around −0.88 V.

$[(Mn_2O_2)_2(tphpn)_2]^{4+}$ exhibits redox potentials which are close to each other [27]. It is an example of a linear tetranuclear oxomanganese cluster with lower oxidation states (II,II,III,III) yielding a stable III,III,III,IV state upon oxidation. In the tacn system [51], one-electron reduction from IV,IV,IV,IV to III,IV,IV,IV is reversible, but a second one-electron reduction leads to an irreversible process. On the other hand, the tacn adamantane complex exhibits an one-electron oxidation from IV,IV,IV,IV to V,IV,IV,IV with a fairly accessible potential (1.32 V(SCE)) [70]. It is the only example of an oxomanganese cluster in which an oxidation state of +5 has been observed on manganese.

The electrochemical behavior of the carboxylato-bridged oxomanganese cluster, $[Mn_4O_2(OOCPh)_7(bpy)]^{2+}$, has also been investigated [62]. This complex shows

four oxidation states, with its lower oxidation state (II,II,III,III) being unstable. This is understandable, as the manganese centers in this complex are supported by bridging carboxylates which stabilize higher oxidation states relative to the lower ones. Oxidation to a III,III,III,IV state is easily attained with a reduction potential of 0.87 V(SCE).

5.3. *Proton-coupled electron transfer*

Thus far, we have discussed electrochemical behavior of oxomanganese clusters in non-aqueous solutions. In aqueous solutions, their behavior reflects interactions with protons/water and, consequently, unusual redox properties have been observed. The interplay of electron transfer concomitant with proton release/uptake is important and relevant to the S-state cycle of the OEC. The Nernst equation [71] for this process is shown below.

$$E = E^0 + (RT/nF)\ \ln([\text{Oxidized}]/[\text{Reduced}]) \tag{2}$$

In the case where

$$\text{Oxidized} + H^+ + e^- \rightarrow [\text{Reduced-H}]^+ \tag{3}$$

Eq. (2) changes to:

$$E = E^0 + (RT/nF)\ \ln([\text{Oxidized}][H^+]/[\text{Reduced}]) \tag{4}$$

where the symbols have their usual meaning, and

$$E = E^0 - 0.0592\{\text{pH} - \log([\text{Oxidized}]/[\text{Reduced}])\} \tag{5}$$

Eq. (5) shows that, for a one-electron, one-proton process, the observed electrochemical potential will vary linearly with the pH (Fig. 11). Various other possibilities also exist, depending on the number of electrons and protons involved in the coupled redox process. This electrochemical potential reflects the thermodynamics of the system, which can be altered by controlling the pH. Protonation/deprotonation at

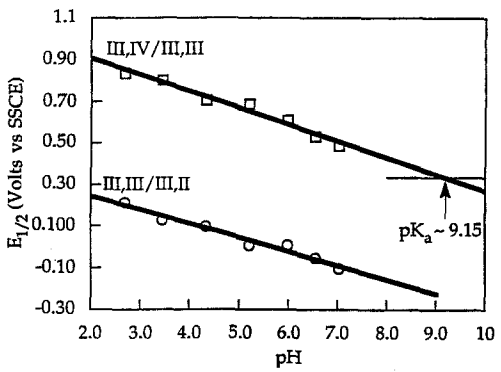

Fig. 11. Pourbaix diagram for $[Mn_2^{III,IV}O_2(phen)_4](ClO_4)_3$ (adapted from, and conditions as in, Ref. [75]).

the oxo-groups of these complexes thus acts as a control over the stabilization of lower/higher oxidation states of the manganese clusters. Oxidation of water involves both electrons and protons, although whether the redox processes in the OEC are proton-coupled is not yet established. But it is clear from model studies that proton-coupled electron transfer (PCET) plays an integral part in tuning the potentials with the change in pH. For example, the electrochemical potentials of $[Mn_2^{III,IV}O_2(bpy)_4]^{3+}$ show a dependence on pH which can be related to Eq. (5). Of the two redox couples exhibited by this complex [72], only the couple around 1.25 V(SCE) exhibits PCET, while the other redox couple is unaffected by the change in the pH. This would suggest the mechanism shown in Eqs. (6a) and (6b):

$$[Mn_2^{III,IV}O_2(bpy)_4]^{3+} + H^+ + e^- \rightleftharpoons [Mn_2^{III,III}(O)(OH)(bpy)_4]^{3+} \quad (6a)$$

$$[Mn_2^{III,III}(O)(OH)(bpy)_4]^{3+} + e^- \rightleftharpoons [Mn_2^{III,II}(O)(OH)(bpy)_4]^{2+} \quad (6b)$$

$[Mn_2^{III,IV}O_2(edda)_2]^-$ (edda = ethylenediamine diacetate) also exhibits a similar mechanism [73]. But this mechanism does not hold for $[Mn_2^{III,IV}O_2(bispicen)_2]^{3+}$; in this case, the electron transfer is decoupled from protonation. This would suggest that at the initial oxidation state (III,IV) the basicity of the bridging oxo-groups is not sufficient for them to be protonated; it is only after reduction to the III,III state that the oxo-group can accept a proton [73]. Baldwin et al. [74] have shown that the pK_a values of a series of $[Mn^{IV}(X\text{-}SALPN)(\mu_2\text{-}O,OH)]_2^+$ complexes, X = 5-OCH_3, H, 5-Cl, 3, 5-diCl and 5-NO_2, track linearly vs. the shift in reduction potential, with a slope of 84 mV pK_a^{-1}. This illustrates an important aspect of proton-coupled electron transfer; the oxidation state of manganese and its ancillary ligands contribute directly to the basicity of the bridging oxo-groups. Changes in these factors result in either coupling or decoupling of proton transfer with a redox process.

Of interest is the aqueous electrochemistry of $[Mn_2^{III,IV}O_2(phen)_4]^{3+}$ [75]. This complex exhibits two reversible redox couples in acetonitrile but, unlike its bpy analogue, this complex undergoes two proton-coupled electron transfers in aqueous solution. Thus, in this case, both of the μ-oxo groups protonate concomitant with electron transfer (Fig. 11).

This observation is of importance because it is the first example of its kind and, moreover, has direct implications on the basicity of oxo-groups. Comparing pK_a values of the μ-hydroxo groups in complexes with bpy (11.0), phen (9.15) and bispicen (8.35), the role of ancillary ligands is clearly seen. It is evident that as the pK_a of the bridging group is decreased, protonation becomes a chemical step following an electron transfer [75]. Protein residues are capable of a similar mechanism by which the pK_a of hydroxo groups in the OEC may be tuned. Subtle changes in the pH around the OEC may thus result in adjustments in the thermodynamics and kinetics of the OEC.

6. Magnetic properties

While electrochemical studies give information about the thermodynamic properties of these complexes, much can be learned about the electronic structure and

exchange interactions by investigations of magnetic properties. Data obtained from temperature-dependent magnetic susceptibility measurements are fit by using different models. The parameters obtained from these fits give an insight into the exchange interactions between different manganese centers. EPR spectroscopic studies are helpful in understanding exchange couplings and give information about the delocalization of d-electrons on different manganese ions. In this section we will discuss magnetic properties of oxomanganese clusters and their relevance to the natural system.

6.1. Electron paramagnetic resonance

Manganese (^{55}Mn) is I=5/2 with its stable oxidation states of +2 (d^5), +3 (d^4), and +4 (d^3). In all the complexes discussed in this text, manganese is high-spin, with all of the d-electrons unpaired. When two or more manganese ions are close to each other, they will couple magnetically. The sign and magnitude of the exchange interactions will depend on the distance between the metal centers, the nature of bridging ligands, and the symmetry of the magnetic orbitals. If the ligand orbitals have the appropriate energies and symmetry, then the exchange interaction may be dominated by superexchange. On the other hand, if the metal ions are close together, their magnetic orbitals may have significant overlap, and the exchange interaction may be dominated by direct exchange.

Several EPR signals are observed from the S_2 state of the OEC (Fig. 3). These EPR signals are indicative of an antiferromagnetically exchange-coupled multinuclear Mn cluster. For di-μ-oxo manganese dimers, only mixed-valent III,IV complexes exhibit EPR signals. In this case, the Mn centers are strongly antiferromagnetically exchange-coupled, resulting in an S=1/2 ground spin state; other oxidation states (III,III; IV,IV) give rise to an EPR-silent S=0 state. For all Mn(III,IV) dimers, a 16-line EPR spectrum centered at $g=2$ (Fig. 12) is diagnostic [76].

There could be two limiting possibilities for the d-electrons: (a) delocalized over both Mn centers, or (b) localized on each Mn center. Crystallographic data on these complexes do not always show distinct metal centers with characteristic bond lengths for Jahn–Teller distorted Mn(III) and non-distorted Mn(IV). Owing to disorder between the two sites, EPR spectroscopy can be used to distinguish between these possibilities.

Considering a delocalized case of an antiferromagnetically exchange-coupled Mn(III,IV) dimer, the spin ground state of S=1/2 would exhibit an EPR signal with an 11-line pattern (2nI + 1; n=2, ^{55}Mn I=5/2), but this is not what is typically observed [31]. For the localized case, hyperfine interactions of $A_{1c}=2A_1$ and $A_{2c}=-A_2$ ($A_1=79$ G; $A_2=83$ G) are obtained (where A_{1c} and A_{2c} are hyperfine coupling constants for the exchange-coupled system; A_1 and A_2 are the hyperfine coupling constants of the uncoupled ions). Each of these hyperfine interactions produces six lines (^{55}Mn I=5/2) resulting in a 16-line pattern with relative intensities of 1:1:2:2:3:3:3:3:3:3:3:3:2:2:1:1 when $A_1=A_2$. For a delocalized case, $A_{1c}=A_{2c}$, and this would give an 11-line pattern with relative intensities of 1:2:3:4:5:6:5:4:3:2:1 (assuming $A_1=A_2$). Thus, the observation of a 16-line

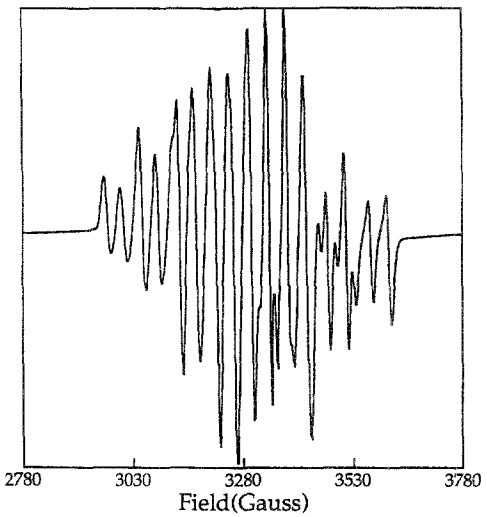

Fig. 12. EPR spectrum from $[Mn_2^{III,IV}O_2(bpy)_4](ClO_4)_3$ in 0.05 M bpy buffer at 15 K; this 16-line EPR spectrum is characteristic of an antiferromagnetically coupled di-μ-oxo manganese (III,IV) complex with trapped valences.

pattern in the EPR signal from a Mn(III)–Mn(IV) species is diagnostic of trapped valences.

Interestingly, EPR characteristics of trinuclear oxomanganese complexes show a distinctive pattern. The basal manganese ions ($Mn^{IV}1$ and $Mn^{IV}2$) are strongly coupled to give a $S=1$ ground spin state with the overall ground spin state (including apical $Mn^{IV}3$) being $S=1/2$. This results in a 35-line EPR spectrum centered at $g=2$. In these cases, the basal manganese ions are treated as a strongly exchange-coupled pair, which are in turn coupled to the apical Mn. Thus, a vector-coupling model [48] in which Mn3 ($I_3=5/2$, $S_3=3/2$) is coupled to the Mn1–Mn2 ($I_{12}=5$, $S_{12}=1$) is valid in this case. This would give the values of hyperfine couplings as $A_{1c}=5/3\ A_3$ and $A_{2c}=-2/3\ A_{12}$ ($A_3=0.0066\ cm^{-1}$ and $A_{12}=0.0061\ cm^{-1}$ with $g=1.965$). For Mn3 a six-line pattern ($2nI+1$; $n=1$, $I=5/2$) is expected, while Mn1–Mn2 give an 11-line pattern ($2nI+1$; $n=1$, $I=5$). With the hyperfine coupling constants calculated above, a 41-line EPR spectrum is expected; hyperfine lines in the spectrum overlap to give a 35-line spectrum (Fig. 13).

A similar treatment using a vector-coupling model can be employed for other higher-nuclearity oxomanganese clusters. It is important, as vector-coupling models can be used to simulate the S_2-state multiline EPR signals, which may be arising from two strongly exchange-coupled manganese dimers that are, in turn, weakly coupled to each other.

For tetrameric oxomanganese clusters, Kirk et al. [77] reported a broad EPR signal centered at $g\approx 6$ for $[(Mn_2^{III,IV}O_2)_2(tphpn)_2]^{4+}$. This signal was observed in parallel polarization mode, implying an integral spin state. In fact, the authors suggest a low-lying $S=1$ spin state. This signal is similar to one observed by

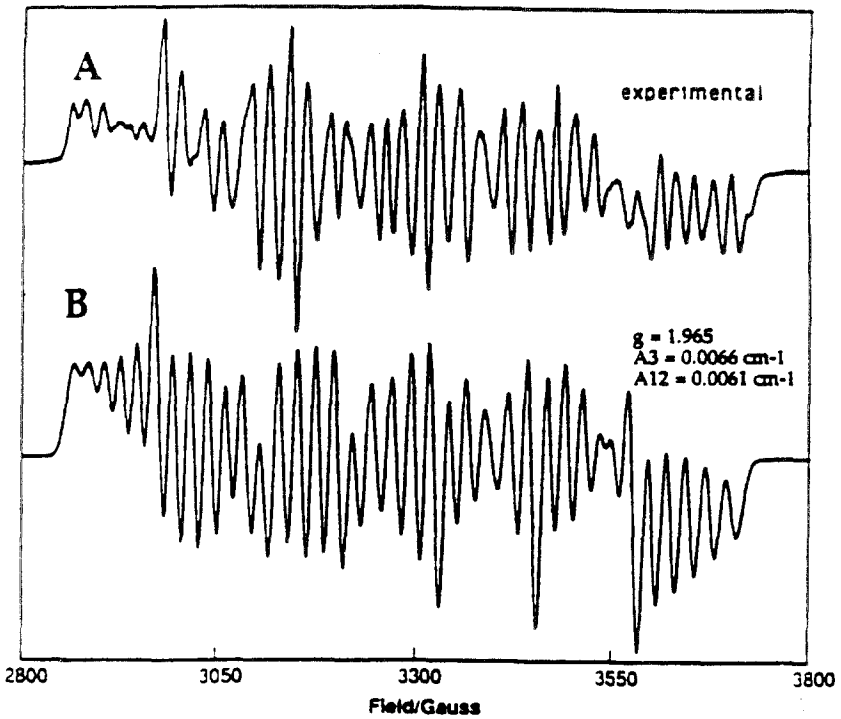

Fig. 13. Experimental and simulated EPR spectra of $[Mn_3^{IV,IV,IV}O_4(bpy)_2(H_2O)_2]^{4+}$. Experimental conditions and parameters for the simulation as in Ref. [48].

Dexheimer and Klein [78] for the S_1 state of the OEC in PS II, although an attempt to reproduce the results of Dexheimer and Klein was unsuccessful [20].

6.2. *Exchange couplings in oxomanganese clusters*

As discussed earlier, the S_2-state multiline EPR signal is attributed to an antiferromagnetically exchange-coupled manganese cluster. To understand the origin and factors affecting this magnetic coupling, inorganic oxomanganese complexes have been used as models (for previous reviews, see Refs. [24,31,32,56]). In a simple case with two Mn centers antiferromagnetically exchange-coupled to each other, the magnetic susceptibility data are fit by using the Heisenberg exchange hamiltonian as in Eq. (7):

$$H_{ex} = J(S_1S_2) \tag{7}$$

The magnitude of J is a direct measure of the exchange coupling between the two metal centers. In di-μ-oxo Mn(III)–Mn(IV) complexes, J values of 250–350 cm^{-1} are typically observed (Table 2). The J value is lower for the Mn(III)–Mn(III) dimers, where $J \approx 200\ cm^{-1}$ is observed; Mn(IV)–Mn(IV) dimers also exhibit couplings in the same range ($J \approx 170$–$230\ cm^{-1}$) (Table 2). The extreme case in this class

is the tri-μ-oxo complex, in which the Mn–Mn distance is shorter than any other dinuclear complex, leading to a much higher value of $J = 770\ cm^{-1}$ [51]. On the other hand, for $[Mn_2^{IV,IV}O_2(pic)_4]^{4+}$ the value of $J = 174\ cm^{-1}$ [79] is much smaller, and for $[Mn_2^{IV,IV}O_2(\mu\text{-}HPO_4)(bpy)_2(H_2PO_4)]$ it is even smaller ($J = 79\ cm^{-1}$) [80]. The weaker antiferromagnetic coupling in these complexes has been attributed to a mostly O-donor environment, resulting in an orbital energy mismatch [79]. However, the orbital symmetry and the distance between the metal centers are also important and are discussed below.

It is possible to analyze the exchange couplings of the dinuclear di-μ-oxo-bridged complexes in more detail because the orbital symmetry of each manganese ion is fixed by the di-μ-oxo coordination (Fig. 9). Based on a consideration of the variation of the exchange interaction with the Mn–Mn distance, Thorp and Brudvig [31] have proposed that direct exchange is significant in di-μ-oxo manganese dimers. This direct exchange mechanism is facilitated by the same orbital symmetry of the occupied d_{xy} orbital on each of the metal centers and the short distance between the two centers. In their model, the observed J values were normalized by taking into account the number of electrons on each Mn. The correlation of this normalized J with the Mn–Mn distance holds well.

There is another aspect of exchange interactions: the orientation of the d_{xy} orbital of each Mn center. For direct exchange, it is required that the orbital overlap be significant. As pointed out by Thorp and Brudvig [31], the d_{xy} orbitals in dinuclear complexes are in a favorable orientation for direct overlap. However, changes in the orientation of the d_{xy} orbitals may result in a different J value. In a simple picture, the dihedral angle between the two O–Mn–O planes would give some idea about the orientation of the d_{xy} orbitals of each Mn. We have used this model to modify the correlation between inter-metal distance and the observed J values for various complexes. We have normalized the observed J value by taking into account the projection of the dihedral angle on the Mn–Mn bond (Table 3). As can be seen in Fig. 14, the normalized J values for these complexes correlate well with the distance between the two Mn centers. This would indicate that even though the number of

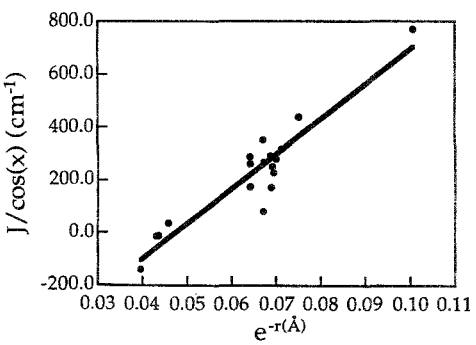

Fig. 14. Correlation of the normalized exchange-coupling parameter $J/\cos(x)$, where x is the angle between the two O–Mn–O planes, with e^{-r}, where r is the Mn–Mn separation in Å for dinuclear oxomanganese dimers.

Table 3
Correlation of observed J values and the angle of the O—Mn—O plane in dinuclear clusters

Complex	Oxidation state	Mn–Mn (Å)	J (cm^{-1})	Dihedral angle (deg)
Di-μ-oxo				
$[Mn_2O_2(6\text{-}Me_2bispicen)_2]^{2+}$	III, III	2.676	172	0.90
$[Mn_2O_2(bispicen)_2]^{3+}$	III, IV	2.659	280	0.00
$[Mn_2O_2(L2)_2]^{3+}$	III, IV	2.702	352.9	0.00
$[Mn_2O_2(phen)_4]^{3+}$	III, IV	2.700	268.1	1.70
$[Mn_2O_2(tmpa)_2]^{3+}$	III, IV	2.643	318	1.10
$[Mn_2O_2(tren)_2]^{3+}$	III, IV	2.679	292.1	0.80
$[Mn_2O_2(bispicen)_2]^{4+}$	IV, IV	2.672	251	0.00
$[Mn_2O_2(bpy)_2(\mu\text{-}HPO_4)(H_2PO_4)_2]^{0}$	IV, IV	2.702	79	11.60
$[Mn_2O_2(L3)_2]^{4+}$	IV, IV	2.747	262	0.00
$[Mn_2O_2(phen)_4]^{4+}$	IV, IV	2.748	288	0.60
$[Mn_2O_2(pic)_4]^{0}$	IV, IV	2.747	174.1	0.00
di-μ-oxo μ-carboxylato				
$[Mn_2O_2(O_2CCH_3)(bpy)_2Cl_2]^{0}$	III, IV	2.667	228	
$[Mn_2O_2(O_2CCH_3)(bpea)]^{3+}$	IV, IV	2.580	248	16.30
$[Mn_2O_2(O_2CCH_3)(tacn)_2]^{2+}$	III, IV	2.588	440	19.09
μ-oxo di-μ-carboxylato				
$[Mn_2O(O_2CCH_3)_2(bpy)_2(H_2O)_2]^{2+}$	III, III	3.132	6.8	0.00 (122.80)[a]
$[Mn_2O(O_2CCH_3)_2(bpy)_2(N_3)_2]^{0}$	III, III	3.153	−6.8	0.00 (125.00)[a]
$[Mn_2O(O_2CCH_3)_2(tmtacn)_2]^{2+}$	III, III	3.084	−18.0	0.00 (120.90)[a]
Tri-μ-oxo				
$[Mn_2O_3(tmtacn)_2]^{2+}$	IV, IV	2.296	770	0.00

[a] The angle in parentheses describes the Mn—O—Mn bend for the μ-oxo di-μ-carboxylato dimers.

electrons on each Mn center and the distance between them are important, the orientation of the d_{xy} orbital of each Mn contributes significantly to the exchange interactions.

In the case of trinuclear complexes, the distance between the basal Mn ions is shorter (about 2.6 Å), while the apical Mn ion is separated from the basal Mn with a longer distance (about 3.2 Å) [28,48,52]. The basal Mn ions are antiferromagnetically exchange-coupled to each other with typical $J = 150$–$180\ cm^{-1}$; on the other hand, the exchange coupling between the basal Mn and the apical Mn is smaller ($J' \approx 100\ cm^{-1}$) (Table 4). To fit the observed magnetic behavior, a vector-coupling model is applied (Fig. 15). This model is based on the difference in exchange interactions between basal and apical Mn centers.

The basal di-μ-oxo Mn unit is strongly antiferromagnetically exchange-coupled with an exchange coupling of J; this antiferromagnetically exchange-coupled dimer is then antiferromagnetically exchange-coupled to the apical Mn with an exchange coupling of J'. In $[Mn_3^{IV,IV,IV}O_4(OH)(bpea)_3]^{3+}$, the exchange coupling, J', is much smaller ($J' = 22\ cm^{-1}$) because the apical Mn is out-of-plane in this complex [52]. As a consequence, a possible disorientation of the occupied d-orbitals along the

Table 4
Inter-metal distances and exchange coupling parameters in trinuclear and tetrameric oxomanganese clusters

Complexes	Oxidation states	Mn−Mn (Å)	Mn−Mn (Å)	J $(cm^{-1})^a$	J' $(cm^{-1})^a$	Ref.
Trinuclear						
$[Mn_3O_4(Cl)_2(bpy)_4]^{2+}$	IV, IV, IV	2.681	3.243	171	108	[61]
$[Mn_3O_4(H_2O)_2(bpy)_4]^{4+}$	IV, IV, IV	2.679	3.254	182	98	[48]
$[Mn_3O_4(OH)(bpea)_3]^{3+}$	IV, IV, IV	2.580	3.2	152	22	[52]
Tetranuclear						
$[Mn_4O_2(O_2CCH_3)_7(bpy)_2]^+$	III, III, III, III	2.845	3.35 (avg)	47	15.6	[62]
$[Mn_4O_3(Cl)_6(O_2CCH_3)_3(HIM)]^{2-}$	III, III, III, IV	2.812 (avg)	3.30 (avg)	na	na	[26]
$[Mn_4O_3(Cl)_4(O_2CCH_3)_3(py)_3]^0$	III, III, III, IV	2.815	3.272	53.6	−24.2	[65]
$[Mn_4O_4(tphpn)_2]^{4+}$	III, III, IV, IV	2.654	3.971	202	16.8	[27]
$[Mn_4O_5(OH)(tacn)_4]^{5+}$	IV, IV, IV, IV	3.250	3.450	45	13.1; 2.7	[35]
$[Mn_4O_5(OH)(tame)_4]^{5+}$	IV, IV, IV, IV	na	na	39.6	19.6; 2.5	[35]
$[Mn_4O_6(bpy)_4]^{4+}$	IV, IV, IV, IV	2.7 (avg)	2.7 (avg)	268	176	[28]
$[Mn_4O_6(tacn)_4]^{4+}$	IV, IV, IV, IV	3.220	3.220	14.5	na	[25]

[a] For trinuclear clusters, $H_{ex}=J(S_1S_2)+J'(S_1S_2+S_2S_3)$; for tetranuclear clusters, exchange parameters for individual clusters have been obtained as described in the text.

Mn(apical)–oxo–Mn(basal) bond may occur, resulting in a weak antiferromagnetic coupling.

Of interest are the magnetic properties of different tetranuclear manganese complexes. Application of a similar vector-coupling model to various classes of tetranuclear clusters yields unique magnetic properties. All butterfly-type complexes show weak antiferromagnetic coupling. There are two different Mn–Mn separations of 2.8 Å and 3.3 Å, which give rise to two different exchange-coupling constants, J and J'. For $Mn_4^{III}O_2(OOCCH_3)_7(bpy)_2]^{2+}$, the exchange values are $J=47\ cm^{-1}$ and $J'=15.6\ cm^{-1}$ [62]. In cubane-type complexes, especially $Mn_4^{III,III,III,IV}O_3Cl_4(OOCCH_3)(py)_3$, two unique exchange-coupling constants are used; J describes the interaction between the three Mn(III)–Mn(IV) units and J' denotes coupling between three Mn(III)–Mn(III) (Fig. 15) [65]. Fitting of the magnetic susceptibility data gives $J=53\ cm^{-1}$ and $J'=-24.2\ cm^{-1}$, implying antiferromagnetic exchange-coupling between Mn(III) and Mn(IV) while Mn(III) and Mn(III) are ferromagnetically coupled. The manganese ions in this case are symmetry-related by a C_3 axis.

For adamantane-type complexes ($[Mn_4^{IV}O_6(L)_4]^{4+}$, (L = tacn or tame)), fitting of the magnetic data was done [25,35] using a second-order hamiltonian, and gave exchange-coupling constants ($J=-13.9\ cm^{-1}$ and $j=-7.8\ cm^{-1}$) indicative of ferromagnetic coupling between Mn(IV) ions. This is an unusual case of a highly symmetric oxomanganese cluster which results in spin frustration. Protonation of the bridging oxo-group relieves this spin frustration by lowering the symmetry of the complex. The second-order treatment is no longer valid and, from fitting the magnetic

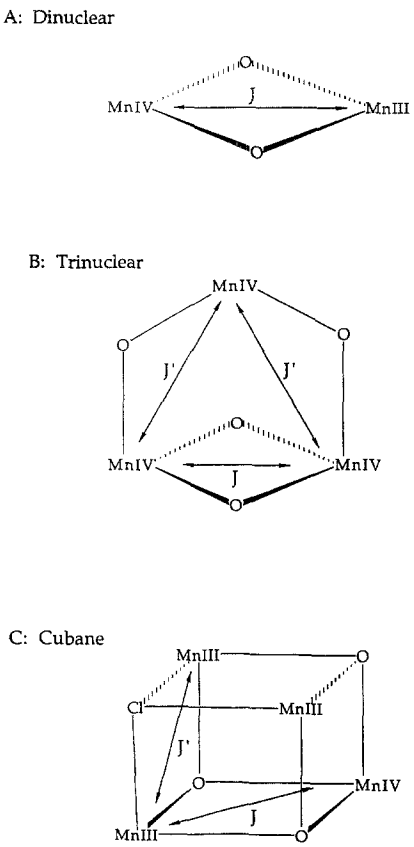

Fig. 15. Exchange couplings in different oxomanganese clusters: A, dinuclear; B, trinuclear; C, cubane. In trinuclear and cubane-type clusters, a vector-coupling model has been used to fit to the magnetic data.

data, three different exchange-coupling constants are extracted, $J_{12}=39.6\ cm^{-1}$, $J_{34}=-2.5\ cm^{-1}$ and $J_{23}=J_{24}=J_{13}=J_{14}=19.6\ cm^{-1}$ [35].

The linear Mn(IV) complex, $[Mn_4^{IV,IV,IV,IV}O_6(bpy)_4]^{4+}$, with four manganese ions bound via three di-μ-oxo units (Fig. 5C), exhibits unique magnetic properties. Magnetic data were fit using a Heisenberg exchange hamiltonian with two distinct coupling constants: $J_{12}=J_{34}=176\ cm^{-1}$ and $J_{23}=268\ cm^{-1}$. The Mn(IV) ions in this complex are antiferromagnetically coupled to give an S=0 ground spin state [28,29]. The spins are assumed to align anti-parallel in order to minimize repulsive interactions, leading to a spin ground state S=0. Another interesting tetranuclear complex, $[(Mn_2^{III,IV}O_2)_2(tphpn)_2]^{4+}$, has been reported [27]. It is a dimer of dimers with two di-μ-oxo Mn(III)–Mn(IV) units linked to each other via two alkoxo bridges. Analysis of its magnetic properties by magnetic susceptibility and isothermal saturation magnetization studies indicate that the two Mn(III)–Mn(IV) di-μ-oxo units are antiferromagnetically coupled ($J=77.6\ cm^{-1}$), resulting in a ground spin state of S=1/2. The overall ground spin state of this complex was found to be S=

1. Instead of a direct exchange mechanism, the authors [77] suggest that the alkoxide bridge mediates an antiferromagnetic exchange coupling, leading to an effective ferromagnetic coupling between the two di-μ-oxo dimers. Further, the authors propose that a change in the oxidation state to the one-electron oxidized form would result in an $S=1/2$ state capable of exhibiting a multiline EPR signal as observed for the S_2 state in PS II. Implications of structural changes in this complex leading to a different ground state have also been analyzed.

7. Conclusions

PS II is a membrane-bound protein which has eluded crystallization so far. Biophysical measurements on this system have given much information for inorganic chemists to model this system. Modeling of the OEC in PS II is a challenge both structurally and mechanistically. We have included in this review research being carried out in this area. We have discussed synthesis, structure, redox properties and magnetism for different classes of oxomanganese clusters. In a simple approach, dinuclear complexes have been studied extensively to understand the behavior of manganese and the bridging oxo-groups. Assembly of higher-nuclearity oxomanganese clusters and subsequent studies on them have given insight into the structure and function of Mn in the OEC. Redox properties of these complexes have been investigated by several electrochemical techniques. The magnetic behavior of oxomanganese complexes is important, as the OEC exhibits distinctive EPR signals associated with its S states. In trying to understand the underlying principles for this behavior, different exchange-coupling models and changes in magnetism, due to either structure changes or protonation, have been put forth. There is still some way to go before the structure of the PS II protein complex can be solved. In the meantime, inorganic chemists will continue to play a key role in providing structural and mechanistic evidence from Mn–oxo clusters to help us understand this complex system.

Acknowledgements

The authors would like to thank Professor J.E. Sarneski (Fairfield University), Professor H.H. Thorp (University of North Carolina) and Professor M. Zimmer (Connecticut College). Helpful discussions with Professor J.P. Caradonna are gratefully acknowledged. This research was supported by the Cooperative State Research Service, United States Department of Agriculture, through agreement No. 90-37130-5575, and the National Institutes of Health (GM 32715).

References

[1] G.W. Brudvig, W.F. Beck and J.C. de Paula, Annu. Rev. Biophys. Biophys. Chem., 18 (1989) 25.
[2] D.F. Ghanotakis and C.F. Yocum, Annu. Rev. Plant Physiol. Plant Mol. Biol., 41 (1990) 255.
[3] A.W. Rutherford, J. Zimmermann and A. Boussac, in J. Barber (ed.), The Photosystems: Structure, Function, and Molecular Biology, Elsevier, Amsterdam, 1992, 179.
[4] R.J. Debus, Biochim. Biophys. Acta, 1102 (1992) 269.
[5] H. Michel and J. Deisenhofer, Biochemistry, 27 (1988) 1.
[6] B. Kok, B. Forbush and M. McGloin, Photochem. Photobiol., 11 (1970) 457.
[7] A.W. Rutherford, Trends Biochem. Sci., 14 (1989) 227.
[8] W.F. Beck, J.C. de Paula and G.W. Brudvig, J. Amer. Chem. Soc., 108 (1986) 4018.
[9] L.I. Krishtalik, Biochim. Biophys. Acta, 849 (1986) 162.
[10] G.W. Brudvig and R.H. Crabtree, Proc. Natl. Acad. Sci. USA, 83 (1986) 4586.
[11] G. Christou and J.B. Vincent, Inorg. Chim. Acta, 136 (1987) L41.
[12] D.M. Proserpio, R. Hoffmann and G.C. Dismukes, J. Am. Chem. Soc., 114 (1992) 4374.
[13] G.N. George, R.C. Prince and S.P. Cramer, Science, 243 (1989) 789.
[14] J.E. Penner-Hahn, R.M. Fronko, V.L. Pecoraro, C.F. Yocum, S.D. Betts and N.R. Bowlby, J. Am. Chem. Soc., 112 (1990) 2549.
[15] V.K. Yachandra, V.J. Derose, M.J. Latimer, I. Mukerji, K. Sauer and M.P. Klein, Science, 260 (1993) 675.
[16] A.-F. Miller and G.W. Brudvig, Biochim. Biophys. Acta, 1056 (1991) 1.
[17] V.J. DeRose, V.K. Yachandra, A.E. McDermott, R.D. Britt, K. Sauer and M.P. Klein, Biochemistry, 30 (1991) 1335.
[18] X. Tang, B.A. Diner, B.S. Larsen, M.L. Gilchrist Jr, G.A. Lorigan and R.D. Britt, Proc. Natl. Acad. Sci. USA, 91 (1994) 704.
[19] B.A. Diner, P.J. Nixon and J.W. Farchaus, Curr. Opin. Struct. Biol., 1 (1991) 546.
[20] G.W. Brudvig, ACS Symposium Series (1995), in press.
[21] J.C. de Paula, J.B. Innes and G.W. Brudvig, Biochemistry, 24 (1985) 8114.
[22] J. Bonvoisin, G. Blondin, J.-J. Girerd and J.-L. Zimmermann, Biophys. J., 61 (1992) 1076.
[23] G.W. Brudvig, ACS Symposium Series, 372 (1988) 221.
[24] G. Christou, Acc. Chem. Res., 22 (1989) 328.
[25] K. Wieghardt, U. Bossek and W. Gebert, Angew. Chem., Int. Ed. Engl., 22 (1983) 328.
[26] J.S. Bashkin, H. Chang, W.E. Streib, J.C. Huffman, D.N. Hendrickson and G. Christou, J. Am. Chem. Soc., 109 (1987) 6502.
[27] M.K. Chan and W.H. Armstrong, J. Am. Chem. Soc., 113 (1991) 5055.
[28] C. Philouze, G. Blondin, S. Ménage, N. Auger, J.-J. Girerd, D. Vigner, M. Lance and M. Nierlich, Angew. Chem., Int. Ed. Engl., 31 (1992) 1629.
[29] C. Philouze, G. Blondin, J. Girerd, J. Guilhem, C. Pascard and D. Lexa, J. Am. Chem. Soc., 116 (1994) 8557.
[30] G.W. Brudvig and R.H. Crabtree, Prog. Inorg. Chem., 37 (1989) 99.
[31] H.H. Thorp and G.W. Brudvig, New J. Chem., 15 (1991) 479.
[32] K. Wieghardt, Angew. Chem., Int. Ed. Engl., 28 (1989) 1153.
[33] W. Levason and C.A. McAuliff, Coord. Chem. Rev., 7 (1972) 353.
[34] K.S. Hagen, W.H. Armstrong and H. Hope, Inorg. Chem., 27 (1988) 967.
[35] K.S. Hagen, T.D. Westmoreland, M.J. Scott and W.H. Armstrong, J. Am. Chem. Soc., 111 (1989) 1907.
[36] B.C. Dave, R.S. Czernuszewicz, M.R. Bond and C.J. Carrano, Inorg. Chem., 32 (1993) 3593.
[37] S.R. Cooper and M. Calvin, J. Am. Chem. Soc., 99 (1977) 6623.
[38] J.B. Vincent, K. Folting, J.C. Huffman and G. Christou, Inorg. Chem., 25 (1986) 996.
[39] B.P. Hay, Coord. Chem. Rev., 126 (1993) 177.
[40] P. Comba, Coord. Chem. Rev., 123 (1993) 1.
[41] H. Frubheis, R. Klein and H. Wallmeier, Angew. Chem., Int. Ed. Engl., 26 (1987) 403.
[42] N.L. Allinger, J. Am. Chem. Soc., 99 (1977) 8127.

[43] R. Brooks, R.E. Bruccoleri, B.D. Olafson, D.J. States, S. Swaminathan and M. Karplus, J. Comput. Chem., 4 (1983) 187.
[44] P.K. Weiner and P.A. Kollman, J. Comput. Chem., 2 (1981) 287.
[45] A.K. Rappé, K.S. Colwell and C.J. Casewit, Inorg. Chem., 32 (1993) 3438.
[46] R. Manchanda, M. Zimmer, G.W. Brudvig and R.H. Crabtree, J. Mol. Struct., 323 (1994) 257.
[47] R. Manchanda, G.W. Brudvig, R.H. Crabtree, J.E. Sarneski and M. Didiuk, Inorg. Chim. Acta, 212 (1993) 135.
[48] J.E. Sarneski, H.H. Thorp, G.W. Brudvig, R.H. Crabtree and G.K. Schulte, J. Am. Chem. Soc., 112 (1990) 7255.
[49] R. Manchanda, G.W. Brudvig and R.H. Crabtree, New J. Chem., 18 (1994) 561.
[50] S. Pal and W.H. Armstrong, Inorg. Chem., 31 (1992) 5417.
[51] K. Wieghardt, U. Bossek, B. Nuber, J. Weiss, J. Bonvoisin, M. Corbella, S.E. Vitols and J. Girerd, J. Am. Chem. Soc., 110 (1988) 7398.
[52] S. Pal, M.K. Chan and W.H. Armstrong, J. Am. Chem. Soc., 114 (1992) 6398.
[53] A. Miller and G.W. Brudvig, Biochemistry, 28 (1989) 8181.
[54] N. Tamura and G. Cheniae, Biochim. Biophys. Acta, 890 (1987) 179.
[55] J.E. Sarneski, M. Didiuk, H.H. Thorp, G.W. Brudvig, R.H. Crabtree and G.K. Schulte, Inorg. Chem., 30 (1991) 2833.
[56] V.L. Pecoraro, Photochem. Photobiol., 48 (1988) 249.
[57] R.M. Fronko, J.E. Penner-Hahn and C.J. Bender, J. Am. Chem. Soc., 110 (1988) 7554.
[58] S. Khangulov, M. Sivaraja, V.V. Barynin and G.C. Dismukes, Biochemistry, 32 (1993) 4912.
[59] U. Bossek, T. Weyhermüller, K. Wieghardt, B. Nuber and J. Weiss, J. Am. Chem. Soc., 112 (1990) 6387.
[60] R.D. Cannon, Prog. Inorg. Chem., 36 (1988) 195.
[61] N. Auger, J.-J. Girerd, M. Corbella, A. Gleizes and J.-L. Zimmerman, J. Am. Chem. Soc., 112 (1990) 448.
[62] J.B. Vincent, H.-R. Chang, K. Folting, J.C. Huffman, G. Christou and D.N. Hendrickson, J. Am. Chem. Soc., 109 (1987) 5703.
[63] R.J. Kulawiec, R.H. Crabtree, G.W. Brudvig and G.K. Schulte, Inorg. Chem., 27 (1988) 1309.
[64] K. Dimitrou, K. Folting, W.E. Streib and G. Christou, J. Am. Chem. Soc., 115 (1993) 6432.
[65] S. Wang, K. Folting, W.E. Strieb, E.A. Schmitt, J.K. McCusker, D.N. Hendrickson and G. Christou, Angew. Chem., Int. Ed. Engl., 30 (1991) 305.
[66] S. Wang, H. Tsai, W.E. Streib, G. Christou and D.N. Hendrickson, J. Chem. Soc., Chem. Comm. (1992) 1427.
[67] C. Gedye, C. Harding, V. McKee, J. Nelson and J. Patterson, J. Chem. Soc., Chem. Comm. (1992) 392.
[68] G.W. Brudvig and J.C. de Paula, in J. Biggins (ed.), Progress in Photosynthesis Research, Vol. 1, Martinus Nijhoff Publishers, The Hague, Netherlands, 1987, p. 491.
[69] S. Yu, C. Wang, E.P. Day and R.H. Holm, Inorg. Chem., 30 (1991) 4067.
[70] T.D. Westmoreland, K.S. Hagen, M.J. Scott and W.H. Armstrong, 1994, personal communication.
[71] A.J. Bard and L.R. Faulkner, Electrochemical Methods Fundamentals and Applications, Wiley, New York, 1980, p. 51.
[72] H.H. Thorp, Chemtracts — Inorganic Chemistry, 3 (1991) 171.
[73] R. Manchanda, H.H. Thorp, G.W. Brudvig and R.H. Crabtree, Inorg. Chem., 30 (1991) 494.
[74] M.J. Baldwin, A. Gelasco and V.L. Pecoraro, Photosynth. Res., 38 (1993) 303.
[75] R. Manchanda, H.H. Thorp, G.W. Brudvig and R.H. Crabtree, Inorg. Chem., 31 (1992) 4040.
[76] G.W. Brudvig, in A.J. Hoff (ed.), Advanced EPR Applications in Biology and Biochemistry, Elsevier, Amsterdam, Netherlands, 1989, p. 839.
[77] M.L. Kirk, M.K. Chan, W.H. Armstrong and E.I. Solomon, J. Am. Chem. Soc., 114 (1992) 10432.
[78] S.L. Dexheimer and M.P. Klein, J. Am. Chem. Soc., 114 (1992) 2821.
[79] E. Libby, R.J. Webb, W.E. Streib, K. Folting, J.C. Huffman, D.N. Hendrickson and G. Christou, Inorg. Chem., 28 (1989) 4037.
[80] J.E. Sarneski, L.J. Brezezinski, B. Anderson, M. Didiuk, R. Manchanda, R.H. Crabtree, G.W. Brudvig and G.K. Schulte, Inorg. Chem., 32 (1993) 3265.

[81] N. Kitajima, U.P. Singh, H. Amagai, M. Osawa and Y. Moro-oka, J. Am. Chem. Soc., 113 (1991) 7757.
[82] P.A. Goodson, A.R. Oki, J. Glerup and D.J. Hodgson, J. Am. Chem. Soc., 112 (1990) 6248.
[83] M.A. Collins, D.J. Hodgson, K. Michelsen and D.K. Towle, J. Chem. Soc., Chem. Comm. (1987) 1659.
[84] P.M. Plaskin, R.C. Stoufer, M. Mathew and G.J. Palenik, J. Am. Chem. Soc., 94 (1972) 2121.
[85] K.J. Brewer, M. Calvin, R.S. Lumpkin, J.W. Otvos and L.O. Spreer, Inorg. Chem., 28 (1989) 4446.
[86] A.R. Oki, J. Glerup and D.J. Hodgson, Inorg. Chem., 29 (1990) 2435.
[87] M. Suzuki, H. Senda, Y. Kobayashi, H. Oshio and A. Uehara, Chem. Lett. (1988) 1763.
[88] M. Stebler, A. Ludi and H.-B. Burgi, Inorg. Chem., 25 (1986) 4743.
[89] D.K. Towle, C.A. Botsford and D.J. Hodgson, Inorg. Chim. Acta, 141 (1988) 167.
[90] J.W. Gohdes and W.H. Armstrong, Inorg. Chem., 31 (1992) 368.
[91] U. Bossek, M. Saher, T. Weyhermuller and K. Wieghardt, J. Chem. Soc., Chem. Comm. (1992) 1780.
[92] S. Ménage, J.-J. Girerd and A. Gleizes, J. Chem. Soc., Chem. Comm. (1988) 431.
[93] J.E. Sheats, R.S. Czernuszewicz, G.C. Dismukes, A.L. Rheingold, V. Petrouleas, J. Stubbe, W.H. Armstrong, R.H. Beer and S.J. Lippard, J. Am. Chem. Soc., 109 (1987) 1435.
[94] F.J. Wu, D.M. Kurtz, K.S. Hagen, P.D. Nyman, P.G. Debrunner and V.A. Vankai, Inorg. Chem., 29 (1990) 5174.
[95] M. Suzuki, S. Tokura, M. Suhara and A. Uehara, Chem. Lett. (1988) 477.